

**CONTROLLED RELEASE OF AMPICILLIN FROM COAXIALLY
ELECTROSPUN POLYCAPROLACTONE NANOFIBERS**

ZAHIDA SULTANOVA

MASTER THESIS

DEPARTMENT OF BIOMEDICAL ENGINEERING

**TOBB UNIVERSITY OF ECONOMICS AND TECHNOLOGY
THE GRADUATE SCHOOL OF NATURAL AND APPLIED
SCIENCES**

DECEMBER 2015

ANKARA

Approval of the Graduate School of Natural and Applied Sciences.

Prof. Dr. Osman EROĞUL

Director

I certify that this thesis satisfies all the requirements as a thesis for the degree of Master of Science.

Prof. Dr. Osman EROĞUL

Head of Department

This is to certify that I have read this thesis and that in my opinion it is fully adequate, in scope and quality, as a thesis for the degree of Master of Science.

Prof. Dr. Mehmet MUTLU

Supervisor

Examining Committee Members

Chair: Assoc. Prof. Dr. Dilek ÇÖKELİLER _____

Member: Prof. Dr. Mehmet MUTLU _____

Member: Asst. Prof. Dr. Cevat ERİŞKEN _____

TEZ BİLDİRİMİ

Tez içindeki bütün bilgilerin etik davranış ve akademik kurallar çerçevesinde elde edilerek sunulduğunu, ayrıca tez yazım kurallarına uygun olarak hazırlanan bu çalışmada orijinal olmayan her türlü kaynağa eksiksiz atıf yapıldığını bildiririm.

I hereby declare that all the information provided in this thesis was obtained with rules of ethical and academic conduct. I also declare that I have sited all sources used in this document, which is written according to the thesis format of the Institute.

Zahida SULTANOVA

University : TOBB University of Economics and Technology
Institute : Institute of Natural and Applied Sciences Science
Programme : Biomedical Engineering
Supervisor : Prof. Dr. Mehmet MUTLU
Degree Awarded and Date : MSc. – December 2015

ZAHIDA SULTANOVA

**CONTROLLED RELEASE OF AMPICILLIN FROM COAXIALLY
ELECTROSPUN POLYCAPROLACTONE NANOFIBERS**

ABSTRACT

Controlled release of hydrophilic biological agents is difficult to be achieved with conventional approaches such as single electrospinning. One recent approach for controlled release is production of core-shell fibers via modified coaxial electrospinning. In this study, the application area of this technique was expanded by using it for a hydrophilic drug (ampicillin) which is known to have low compatibility with polycaprolactone (PCL). A partially electrospinnable 4% (w/v) PCL solution was used as a shell fluid in order to create ampicillin-loaded PCL nanofibers shelled by a PCL shield. Scanning electron microscopy and optical microscopy verified that the membranes consisted of nanofibers with core-shell structure. Furthermore, Fourier transform infrared spectroscopy demonstrated that some compatibility might be present between ampicillin and PCL. Finally, drug release studies showed that the drug release kinetics of core-shell products is closer to zero-order kinetics as compared to the products of single electrospinning. Together, these imply that the application area of modified electrospinning in controlled release could be expanded to polymers and drugs with low compatibility.

Keywords: Controlled release, Coaxial electrospinning, Drug release membrane, Polycaprolactone, Ampicillin

Üniversitesi : TOBB Ekonomi ve Teknoloji Üniversitesi
Enstitüsü : Fen Bilimleri Enstitüsü
Anabilim Dalı : Biyomedikal Mühendisliği
Tez Danışmanı : Prof. Dr. Mehmet MUTLU
Tez Türü ve Tarihi : Yüksek Lisans – Aralık 2015

ZAHIDA SULTANOVA

**ORTAK EKSENLİ ELEKTROEĞİLMİŞ POLİKAPROLAKTON
NANOFİBERLERDEN AMPİSİLİNİN KONTROLLÜ SALIMI**

ÖZET

Hidrofilik biyolojik ajanların kontrollü salımını gerçekleştirecek ortamların oluşturulmasında tekli elektro-eğirme gibi geleneksel yöntemler yetersiz kalmaktadır. Kontrollü salım için öne sürülen yaklaşımlardan biri modifiye ortak eksenli elektro-eğirme yöntemi ile kabuk-çekirdek biçiminde fiberler üretimidir. Bu çalışmada, hidrofilik ve model polimerle uyumluluğu az olan bir ilaç kullanılarak, bahsedilen yöntemin kullanım alanı genişletilmiştir. Polikaprolakton (PCL) ile kaplanmış ampisilin içeren PCL nanofiberlerinin üretimi için kısmen elektro-eğrilebilen %4 (ağırlık/hacim) polikaprolakton çözeltisi kabuk sıvısı olarak kullanılmıştır. Taramalı elektron mikroskopu ve optik mikroskop sonuçları ile membranların kabuk-çekirdek biçiminde nanofiberlerden oluştuğu kanıtlanmıştır. Fourier dönüşümlü kızılötesi spektroskopisi ile ampisilin ile PCL arasında az miktarda uyumluluk olabileceği gözlenmiştir. Son olarak ilaç salım çalışmalarında kabuk-çekirdek biçimindeki membranlardan ilaç salımının tekli elektro-eğrilmiş membranlara göre sıfırıncı dereceden kinetik denkleme daha uygun olduğu saptanmıştır. Bu sonuçlar ışığında modifiye ortak eksenli elektro-eğirme yönteminin ilaç salımındaki kullanım alanının uyumluluğu az olan polimer ve ilaçlar için genişletilebileceği görülmüştür.

Anahtar Kelimeler: Kontrollü salım, Çift eksenli elektro-eğirme, İlaç salım membranı, Polikaprolakton, Ampisilin

ACKNOWLEDGEMENT

I would like to thank:

My supervisor Prof Dr. Mehmet Mutlu for his support during my research,
Prof. Dr. Osman Erođul, who always has time for his students despite being extremely busy,

TOBB University of Economics and Technology for supporting me as a full-scholarship student,

Assoc. Prof. Dr. Dilek ökeliler and Assist. Prof. Dr. Cevat Erişken for accepting to be a part of my thesis committee,

Assoc. Dr. Gökhan Barış Bağcı who showed me how a person can be both humble and sophisticated in addition to being a successful scientist,

Prof Dr. Güler Somer for reminding me never to forget our ancestors,

My family who lighten every path I take,

Emel and all my friends from METU where I spent my happiest four years,

Yasemen, Çağla and Didem for proving me that the closest friends can even be found in a one month internship,

Gizem, Emre, Ümit and Gözde who made my “Friday Nights” joyful,

And finally Prof. Dr. Engin Arık whose ideas and curiosity for science was and will always be with me during my academic career.

The thesis is dedicated to my three sisters Lale, Nermin and Esmer.

TABLE OF CONTENTS

Title	Page
ABSTRACT	iv
ÖZET.....	v
ACKNOWLEDGEMENT	vi
TABLE OF CONTENTS	vii
LIST OF TABLES	x
LIST OF FIGURES	xi
LIST OF ABBREVIATIONS	xii
1. INTRODUCTION.....	1
1.1. Introduction and Aim	1
2. LITERATURE REVIEW.....	3
2.1. Controlled Release Principles	3
2.2. Controlled Release Mechanisms	4
2.2.1. Diffusion-controlled release.....	5
2.2.2. Swelling-controlled release	7
2.2.3. Chemically-controlled release.....	8
2.3. Electrospinning	9
2.3.1. Working Principle of Electrospinning	9
2.3.2. Parameters Affecting Electrospinning	10
2.3.2.1. Process Parameters.....	11
2.3.2.2. Material Parameters	11
2.3.2.3. Ambient Parameters	12

2.3.3. Types of Electrospinning	12
2.4. Coaxial Electrospinning	14
2.4.1. Working Principle of Coaxial Electrospinning	14
2.4.2. Coaxially Electrospun Nanofibers for Drug Delivery Applications	16
2.4.3. Modified Coaxial Electrospinning	18
2.5. Characterization Techniques	19
2.5.1. Scanning Electron Microscopy (SEM).....	19
2.5.2. Optical Microscopy	19
2.5.3. Fourier Transform Infrared Spectroscopy (FTIR)	20
2.5.4. Ultraviolet–visible spectroscopy (UV-Vis Spectroscopy).....	20
3. MATERIALS AND METHODS	21
3.1. Materials.....	21
3.2. Methods.....	21
3.2.1. Optimization Studies for Core and Shell Solutions	21
3.2.1.1. Optimization of Electrospinning Parameters	22
3.2.1.2. Electrospinnability of Solutions with Different PCL Concentrations.....	23
3.2.2. Coaxial Electrospinning and Production of Membranes	23
3.2.3. Characterization of the Membranes	27
3.2.4. Drug Release Studies	28
3.2.5. Statistical Analysis	29
4. RESULTS AND DISCUSSION	31
4.1. Results of the Preliminary Studies	31
4.2. Taylor Cone Formation in Coaxial Electrospinning	35
4.3. Morphology and Structure of Nanofibers	37

4.4. Compatibility of Components	44
4.5. In vitro drug release profiles	46
5. CONCLUSION AND FUTURE STUDIES	51
REFERENCES	53
APPENDIX	60
CURRICULUM VITAE.....	67

LIST OF TABLES

Table	Page
Table 3.1. Electrosopinning parameters investigated in the preliminary studies.....	22
Table 3.2. Flow rates used for production of samples	25
Table 4.1. Electrospinning parameters used for production of membranes.....	36

LIST OF FIGURES

Figure	Page
Figure 2.1. Schematic illustration of vertical electrospinning setup	10
Figure 2.2. Schematic illustration of (A) emulsion electrospinning and (B) coaxial electrospinning	13
Figure 2.3. Schematic illustration of coaxial electrospinning setup	15
Figure 2.4. Formation of Taylor cone	16
Figure 3.1. Coaxial electrospinning nozzle.....	24
Figure 3.2. Sketch of a coaxial nozzle	26
Figure 3.3. Picture illustrating the formation of core-shell nanofibers in the study ..	27
Figure 3.4. Photograph of coaxial electrospinning system used in the study.....	27
Figure 3.5. Calibration curve indicating the relationship between absorbance and ampicillin concentration in PBS.....	29
Figure 4.1. Photograph of a stable Taylor cone	31
Figure 4.2. Electrospinning product of 3% (w:v) PCL	33
Figure 4.3. Electrospinning product of 4% (w:v) PCL	34
Figure 4.4. Electrospinning product of 5% (w:v) PCL	34
Figure 4.5. Higher magnification of 4% (w:v) PCL electrospinning product	35
Figure 4.6. Taylor cone formation during coaxial electrospinning.....	36
Figure 4.7. Fiber diameter distributions of the membranes	38
Figure 4.8. SEM image of CR membrane with (a) 2500X, (b) 5000X, (c) 20000X and (d) 50000X magnification	38
Figure 4.9. SEM image of CS1 membrane with (a) 2500X, (b) 5000X, (c) 20000X and (d) 50000X magnification	39
Figure 4.10. SEM image of CR membrane with (a) 2500X, (b) 5000X, (c) 20000X and (d) 50000X magnification	40
Figure 4.11. SEM image of shell electrospinning with (a) 2500X and (b) 5000X magnification.....	41
Figure 4.12. SEM image of a microparticle surface produced by shell electrospinning	41
Figure 4.13. Core-shell structure of CS1 membrane.....	43
Figure 4.14. Core-shell structure of CS2 membrane.....	43
Figure 4.15. Molecular structures of (a) ampicillin and (b) PCL.....	44
Figure 4.16. ATR-FTIR spectra of the Ampicillin, PCL and electrospun membranes	45
Figure 4.17. In vitro drug release profiles of Core/Shell 1, Core/Shell 2 and Core membranes in first 4 hours.....	47
Figure 4.18. In vitro drug release profiles of Core/Shell 1, Core/Shell 2 and Core membranes (full range).....	47
Figure A.1. Schematic illustration of the drug concentration - distance profile of the matrix exposed at time t and t + dt.....	57

LIST OF ABBREVIATIONS

Abbreviation	Definition
ANOVA	Analysis of Variance
FTIR	Fourier Transform Infrared Spectroscopy
HSD	Honest Significant Difference
PBS	Phosphate Buffered Saline
PCL	Polycaprolactone
SEM	Scanning Electron Microscope
UV	Ultraviolet
VIS	Visible

1. INTRODUCTION

1.1. Introduction and Aim

Electrospinning is a technique in which high voltage is used in order to overcome the surface tension of polymer solutions which results with nano/micro-scaled fibers [1]. The nanofibers produced by this process have controllable membrane thickness, large surface area to volume ratio, and can be used as membranes after they are randomly assembled [2]. These membranes have applications in several fields including filtration, tissue engineering, pharmaceuticals and drug delivery [3-8]. In drug delivery applications, various controlled drug release profiles (delayed, immediate, sustained etc.) can be achieved by using electrospun nanofibrous membranes as carriers [9, 10]. Sustained drug release has attracted significant attention among them because it can lead to desired duration and dosage of drugs in target tissues [11].

In order to prepare a drug-loaded nanofibrous membrane, the model drug should be dissolved together with the polymer and then electrospun under appropriate processing conditions. In such membranes, the initial burst release is unavoidable due to the drug distribution on the surface of the nanofibers, large nanofiber surface areas, and amorphous status of the drugs inside the nanofibers [12, 13]. One way to eliminate the burst release is post-treatment of membranes applied after electrospinning. The ones generally used for electrospun membranes are cross-linking or chemical modifications. Unfortunately, both types of post-treatments have an inevitable problem of reduced biocompatibility [14, 15]. Another way of eliminating the burst release is using coaxial electrospinning technique for encapsulating the drugs inside the core of the core-shell structured nanofibers [16].

Coaxial electrospinning is superior to the usage of post-treatment steps as it decreases the complexity of the process and eliminates the potential damage that could be caused by post-treatment. On the other hand, the shell solution used in traditional coaxial electrospinning should be highly electrospinnable and have

enough viscosity for overcoming the interfacial tension between core and shell fluids [13].

Recently, a modification was made on traditional coaxial electrospinning, where dilute polymer solutions or organic solvents were used as shell fluids despite being unspinnable. Literature review reveals that, firstly organic solvents were used as shell fluid in order to control the nanofiber diameters [17, 18]. Next, dilute polymer solutions were used as shell fluid for producing a sustained drug release membrane. The model drug chosen (ketoprofen) in those studies was hydrophobic, miscible in the solvents and had good compatibility with the chosen polymers (zein and cellulose acetate) [19, 20]. Compatibility refers to the interactions between the drug and the polymer which do not cause any alteration in the chemical structure of the polymer or the drug. As every drug has different chemical and physical properties, it is impossible to produce a drug release membrane from a particular polymer which will be suitable for carrying all kinds of drugs [21].

In this research, modified coaxial electrospinning was used for controlled release of a hydrophilic drug, ampicillin, which is known to have low compatibility with the chosen polymer, polycaprolactone. The results of this research have shown that, the application area of modified electrospinning in controlled release could be expanded to polymers and drugs with low compatibility.

2. LITERATURE REVIEW

2.1. Controlled Release Principles

Controlled drug release is one of the most rapidly advancing areas in science. Knowledge of biology, chemistry and material science is essential for working in this field. The controlled drug release systems are generally more advantageous than the conventional dosage forms as they have improved efficacy and reduced toxicity. Synthetic polymers are often used in those systems as drug carriers. The common denominator of controlled release systems is to improve the effectiveness of drug therapy. Compatibility between a drug and its carrier (polymers, liposomes etc.) is one of the essential factors, which influence the effectiveness of controlled drug delivery systems. Primary interactions refer to strong bonds such as ionic, covalent and metallic bonds [22]. Compatibility mainly refers to secondary interactions between drugs and their carriers. They are weaker as compared to secondary interactions. There are several types of it [21, 23]:

Ionic interactions: It happens between ions or molecules with full permanent charges that arise from the attraction between a cation (positively charged ion) and an anion (negatively charged ion). The bonds between them cannot be considered covalent as the electrons are not shared.

Van der Waals forces: They are caused by non-uniform charge distributions on different atoms. The momentary random fluctuations in the electron distributions of an atom result in formation of a dipole. It includes London dispersion force, dipole-induced dipole interaction and dipole-dipole interaction. Dipole-dipole interaction is the one, which happens between permanent dipoles in molecules. Dipole-induced dipole interaction is the one, which occurs between a non-polar molecule without permanent dipole and a molecule with a permanent dipole. In this type of interaction, a non-polar molecule becomes “induced” dipole upon polarization toward or away from a permanent dipole molecule. Finally, London dispersion force is the one that occurs between two induced dipoles.

Hydrogen bonding: It is a special kind of a dipole-dipole attraction that occurs between a highly electronegative atom (sulfur, oxygen, fluorine, or nitrogen atom) and hydrogen atom which is partially positive.

Hydrophobic interactions: It takes place between nonpolar molecules, which do not contain a dipole moment or any ions. It is the tendency of nonpolar molecules to aggregate in aqueous solution where water molecules are excluded [23].

Drug release in the systems can be controlled temporally, spatially or both. The temporal control is achieved by protection of drug molecules against being quickly dissolved inside the aqueous environment of the patient. It involves inhibition of drug diffusion or delay of drug dissolution. Extended duration of release is beneficial if drugs that are rapidly metabolized and eliminated from the body are used. The spatial control on the other hand, is achieved by targeting the release of the drug to a certain site within the body. It can simply be done by implanting the drug release system topically [24]. Tissue scaffolds can be appropriately utilized as drug delivery systems. These scaffolds can facilitate the delivery of drugs while helping tissue growth and providing structural support [25]. For obtaining temporal and spatial control, controlled release mechanisms should be investigated thoroughly.

2.2. Controlled Release Mechanisms

Several mechanisms are involved in the release process. Understanding those mechanisms and identifying the main parameters affecting them are important for designing drug delivery systems. During the drug release process, usually more than one mechanism is involved. Moreover, during different stages, different mechanisms might dominate [26]. Those mechanisms can be degradation of covalent bonds, swelling, reversible drug–polymer interactions or diffusion [27].

2.2.1. Diffusion-controlled release

If the matrix used for drug release is porous and the molecular dimensions of the drug is much smaller than the pore sizes, the diffusion coefficient plays significant role. On the other hand, if the matrix is non-porous or the pore sizes are small, drug diffusion coefficient decreases due to increased drug diffusion path length.

If the system includes a drug encapsulated inside a polymer and the system is in steady state, Fick's first law of diffusion can be used for describing the release profile through the membrane (see Appendix for derivation):

$$J = - D \times \frac{dC}{dx} \quad (2.1)$$

where J (mol/(m²s)) is the flux of the drug, D (m²/s) refers to the diffusion coefficient, x (m) is the position and C (mol/m³) is the concentration of drug.

If the system includes a drug entrapped inside a polymer, the drug is uniformly dispersed, and the drug concentration changes with time, Fick's second law of diffusion can be used for describing the release profile (see Appendix for derivation) [27]:

$$\frac{\partial c}{\partial t} = D \frac{\partial^2 c}{\partial x^2} \quad (2.2)$$

where x (m) is the position, D (m²/s) refers to the diffusion coefficient, t (s) is time and C (mol/m³) is the concentration of drug [27].

If the drug release rate from a system does not depend on its concentration, zero order kinetics equation can be used. The zero order drug release equation is (see Appendix for derivation) [28]:

$$(2.3)$$

$$C = C_0 + K_0t$$

Where Q (mol/m^3) is the amount of released drug, Q_0 (mol/m^3) refers to the initial amount of drug inside the medium (which is usually zero), K_0 ($\text{mol}/(\text{m}^3\text{s})$) refers to the zero order release constant and t (s) is the time [28].

If the drug release rate from a system depends on its concentration, first order kinetics equation can be used. The first order drug release equation is (see Appendix for derivation) [29]:

$$\log(C) = \log(C_0) + Kt/2.303 \quad (2.4)$$

Where Q (mol/m^3) is the amount of released drug, Q_0 (mol/m^3) is the initial amount of drug inside the medium, t (s) is the time and K (s^{-1}) refers to the first order release constant [29].

Higuchi equation can be used for describing the release profile by diffusion (see Appendix for derivation) [30]:

$$\frac{M_t}{M_\infty} = K_H \times t^{1/2} \quad (2.5)$$

Where M_t (mol/m^3) is the amount of drug released up to a certain time t (s), M_∞ (mol/m^3) refers to the final amount of drug released and K_H ($\text{s}^{-1/2}$) is Higuchi constant [30].

Later, Korsmeyer-Peppas equation was proposed for describing the release profile by diffusion:

$$\frac{M_t}{M_\infty} = k \times t^n \quad (2.6)$$

Where M_t (mol/m^3) is the amount of drug released up to a certain time t (s), M_∞ (mol/m^3) refers to the final amount of drug released; n is the release exponent indicating the mechanism of drug release and k (s^{-n}) is a structural/geometric constant for a certain system. There are different n values for drug release matrices with distinct release mechanisms and geometries [27]. The assumptions for the application of the Peppas equation are homogeneously distribution of the drug on the carrier matrix, perfect sink conditions and constant diffusivity [20, 31].

Several factors affect the rate of drug release controlled by diffusion. The first one is the presence of primary or secondary interactions between the drug and the polymer. The second one is how easy the medium can penetrate the matrix. The final one is drug dissolvability in the release medium [32].

2.2.2. Swelling-controlled release

Polymers used in drug delivery systems might have a swelling-driven phase transition from a glassy state to a rubbery state. In the rubbery state, the drug molecules diffuse rapidly; however, in the glassy state the drug molecules are immobile. If such a system is present, the release profile depends on the rate of gel swelling. If the system is diffusion-controlled the time-scale of drug diffusion is the rate-limiting, on the other hand, if the system is a swelling-controlled polymer, then the relaxation (λ) is the rate limiting step.

If both diffusion-controlled and swelling-controlled release is present, a modification of Peppas equation can be used [27]:

$$\frac{M_t}{M_\infty} = k_1 t^m + k_2 t^{2m} \quad (2.7)$$

In the equation, M_t (mol/m^3) is the amount of molecule released up to any time t (s), M_∞ (mol/m^3) is final amount of molecule released, k_1 (s^{-m}), k_2 (s^{-2m}) and m are

constants; $k_1 t^m$ represents diffusion contribution and $k_2 t^{2m}$ represents polymer relaxation contribution to the release profile [27].

2.2.3. Chemically-controlled release

Diffusion and swelling controlled release mechanisms are mainly for drugs that have the same polarity as the medium which is generally aqueous. If the drug does not dissolve in the release medium, the primary driving force for drug release is considered to be chemically controlled degradation of the polymer [32].

Chemically-controlled delivery can be further divided into two types:

Kinetic-controlled release: in this mechanism, diffusion is assumed to be negligible and polymer degradation is the rate-determining step

Reaction-diffusion-controlled release: in this mechanism diffusion is not negligible. Both diffusion and reaction is included in the model [27].

Hopfenberg equation can be used for describing the release profile by matrix erosion. It can be used for the release profile from surface eroding cylindrical matrices with an initial dimension a_0 [27]:

$$\frac{M_t}{M_\infty} = 1 - \left(1 - \frac{k_a t}{C_0 a_0}\right) \quad (2.8)$$

where, M_t (mol/m^3) is the amount of molecule released up to any time t (s), M_∞ (mol/m^3) is final amount of molecule released. n is a geometrical factor which is 2 for cylindrical shape and 3 for spherical shape, C_0 is the drug concentration and k_a is the degradation constant [27].

2.3. Electrospinning

Electrospinning is one of the methods used for fabricating fibrous drug release systems. It uses electric force in order to draw charged threads of polymer solutions up to nanoscale fiber diameter. The process does not need any further wet-chemical treatment or high temperature for the formation of nanofibers [1].

2.3.1. Working Principle of Electrospinning

In this method, a high voltage is applied to a liquid droplet. The liquid droplet consists of a polymer solution or polymer melt. The voltage should be high enough so that electrostatic repulsions (between like charges inside the solution) and electrostatic attraction (between the oppositely charged collector and liquid droplet) can overcome the surface tension. This will result with Taylor Cone formation from a rounded meniscus on the needle tip. From the Taylor cone, a fiber jet is ejected and the solvent, if involved, evaporates during the travel of the jet. As a result, solid polymer nanofibers are deposited on the collector. Straightforward production of biomaterials at this scale caused an interest in electrospinning in tissue engineering and drug delivery applications [33, 34].

In Figure 2.1, a vertical setup of an electrospinning system is shown. The components of the system include:

Voltage supply: The applied voltage is adjusted with the voltage supply.

Grounded target (also called the collector): It is where the fibers are collected. It should be made from a conductive material.

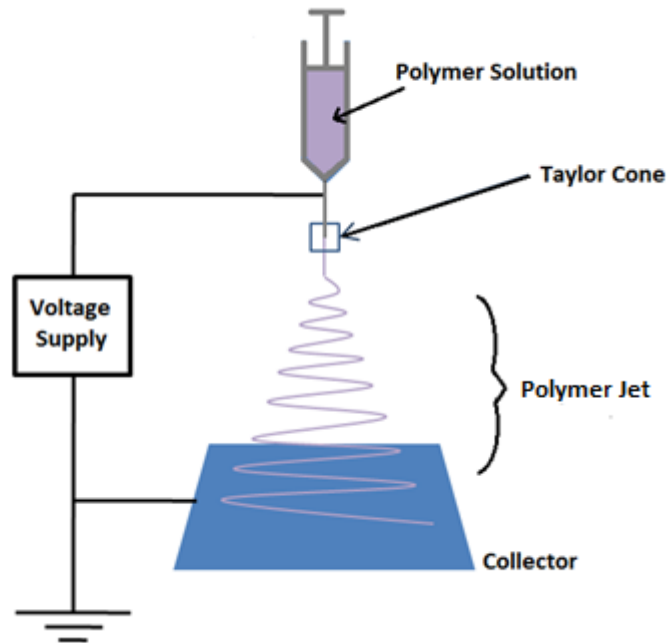


Figure 2.1. Schematic illustration of electrospinning setup

Syringe: The polymer solution is drawn into the syringe. Then, it is placed inside a syringe pump which automatically adjusts the pumping force for a particular flow rate. The Taylor cone and the liquid jet are formed when the electrospinning process begins [2].

2.3.2. Parameters Affecting Electrospinning

There are three types of parameters affecting the electrospinning process: Process parameters, Material parameters and Ambient parameters.

2.3.2.1. Process Parameters

Process parameters affecting the quality of fibers are:

Electrical Potential: Firstly, the voltage applied to the liquid droplet affects the formation of Taylor cone. When it is lower than the critical voltage, Taylor cone and the jet is not formed properly. When it is much higher than the critical voltage, the Taylor cone becomes unstable and bead formation occurs. Secondly, it was observed that fiber diameter decreases with increasing voltage [35].

Flow Rate: If flow rate is too high than plugging of needle tip can be observed due to excess polymer solution. Also, it should be sufficient for fiber production [35].

Distance between the capillary and collection screen: The decrease in fiber diameter is observed with increase in distance. However, if beads are present, increase in distance caused larger beads on the fibers [36].

Needle gauge: It affects the Taylor cone formation parameters (critical voltage and tip to collector distance) [37].

Type of the collector: There are several types of collectors, which act as the conductive surface for collecting the fibers. Plane plate collector, drum rotatory collector and grid type collector are some of them. It was found that the shape and size of the collector has an effect on alignment, diameter and structure of the nanofibers produced during electrospinning [38].

2.3.2.2. Material Parameters

Polymer concentration: increase in polymer concentration is found to increase the diameters of the fibers that are produced. Also, it was found that formation of fibers can be blocked due to the high viscosity of the solution at high polymer

concentration. If the concentration of the solution is too low, nanoparticles were observed instead of nanofibers [35].

Molecular weight of the polymer: it was observed that fiber diameter increases with molecular weight of the polymer. Also, when low molecular weight was used, the fibers are found to have circular cross-section. On the other hand, at high molecular weights flat fibers were observed [39].

Also, viscosity, conductivity and surface tension of the solution all affect the electrospinning process and they should be between certain ranges for stable Taylor cone formation. These ranges change for different polymer solutions. Viscosity and surface tension can be regulated by using different ratios of solvents. Conductivity is mostly affected by solvent and polymer types [40, 41].

2.3.2.3. Ambient Parameters

Ambient parameters affecting the fiber quality are humidity, temperature and air velocity in the chamber. Evaporation rate of the solvent increases with increase in temperature, on the other hand, viscosity decreases with increase in temperature. Effect of humidity on fiber diameter depends on the chemical and molecular interactions of the polymer and solution. In general ambient conditions should all be kept constant for uniform fiber production [42].

2.3.3. Types of Electrospinning

Single Electrospinning: It is the conventional electrospinning where one nozzle and one syringe pump is used.

Coaxial Electrospinning: In this type of electrospinning a core–shell nozzle is attached to a supply of two polymer solutions. One syringe pump is for shell polymer solution and the other is for core polymer solution. As a result, its setup is more complicated than single electrospinning setup which includes a single nozzle and syringe pump.

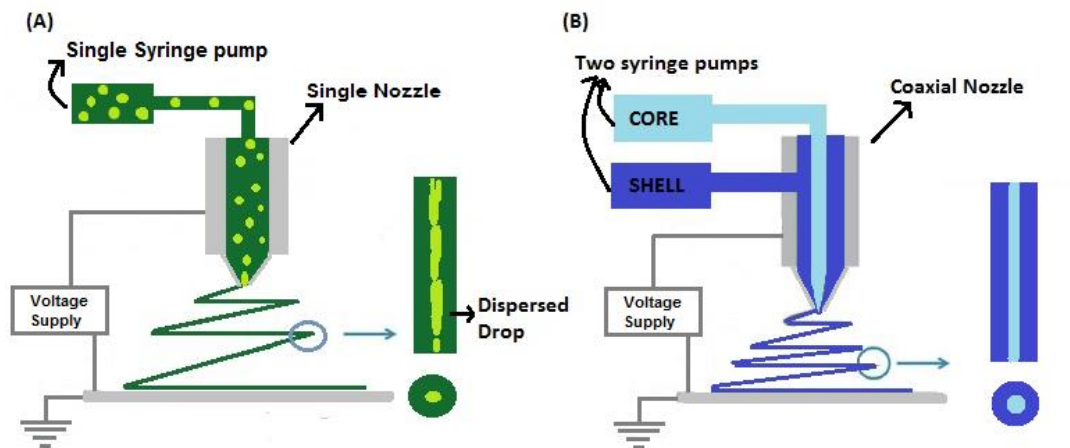


Figure 2.2. Schematic illustration of (A) emulsion electrospinning and (B) coaxial electrospinning (modified from reference [43])

Emulsion Electrospinning: It is demonstrated that production of core–shell polymer nanofibers is also possible by using single electrospinning setup. For this, an emulsion of two polymer solutions should be prepared as a working liquid [44]. In figure 2.2, emulsion electrospinning and coaxial electrospinning are schematically illustrated. In emulsion electrospinning, a single nozzle is used; however, in coaxial electrospinning a coaxial nozzle with two capillaries is needed. The core and shell solution of emulsion electrospinning should not be miscible so that they can form the emulsion. On the other hand, for coaxial electrospinning both miscible and immiscible core and shell solutions can be used.

Melt Electrospinning: In this type, polymer melts are used instead of dissolving the polymers inside volatile solvents [45]. Although it is an alternative to solution

electrospinning, it has generally caused the formation of fibers with diameters of tens of microns [46, 47].

2.4. Coaxial Electrospinning

2.4.1. Working Principle of Coaxial Electrospinning

The general set up of coaxial electrospinning is quite similar to that used for single electrospinning. The modification is made in the spinneret. A smaller inner capillary is inserted into a bigger capillary to obtain the co-axial configuration. The two capillaries are adjusted to fit concentrically. The outer capillary is connected to the syringe containing the shell solution, and the inner one is attached to a second syringe containing the core solution [13]. Two polymer solutions are coaxially electrospun through different channels in order to synthesize core-shell structured nanofibers [48]. Core and shell solutions are distinctly prepared and put into different syringe pumps. The flow rates of each solution can be adjusted during the process for formation of stable Taylor cone. All the other features (voltage, collector-needle distance etc.) are adjusted similar to what is done in traditional single electrospinning setup. The arrangement of the setup can be horizontal or vertical [49].

A typical coaxial electrospinning setup is illustrated in Figure 2.3. It can be seen from the figure that the general components of the setup (high voltage supply, grounded electrode) are similar to single electrospinning but the spinneret is more advanced due to the presence of two different capillaries [13].

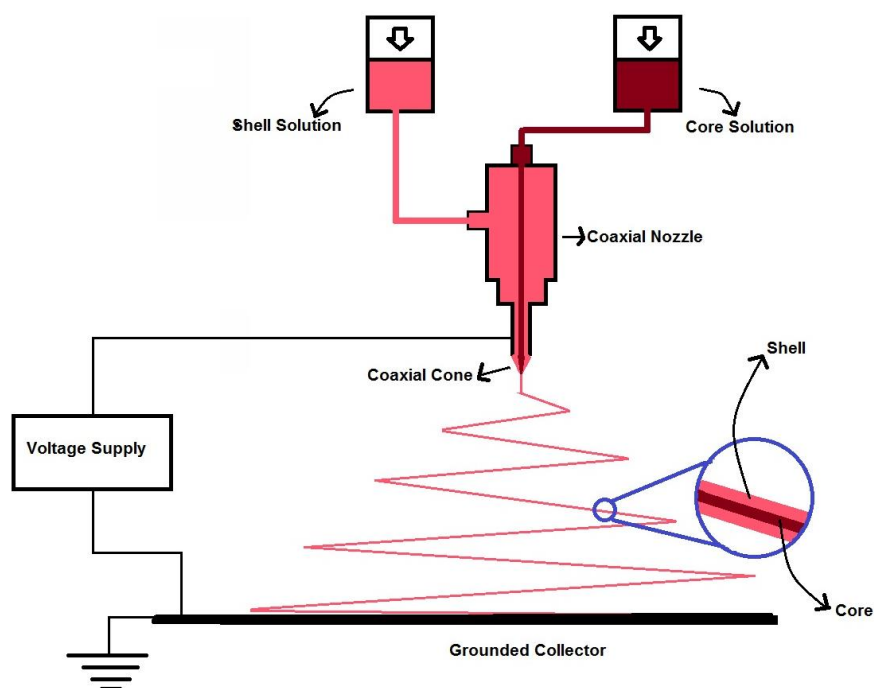


Figure 2.3. Schematic illustration of coaxial electrospinning setup (modified from reference [13])

For coaxial electrospinning, many different polymers were used by other investigators. Those polymers include natural materials, synthetic materials, and synthetic biodegradable polymers. The electrospinning products were then used as drug delivery devices, tissue engineering scaffolds and wound dressings. In addition to biomedical applications those products were also used as liquid, gas, and molecular filters, in photovoltaic, LCD devices, thermomechanical and biochemical sensor devices [13].

Interaction between the core and the shell solutions is essential for coaxial electrospinning. Firstly, the solvent in both the core and shell solutions should not precipitate the polymer from the other one when the two solutions meet at the needle tip [50]. Secondly, the interfacial tension between the core and shell solutions should be as low as possible so that the compound Taylor cone will be stable [51]. In Figure

2.4, a drawing for illustration of Taylor cone formation on the coaxial needle tip is shown.

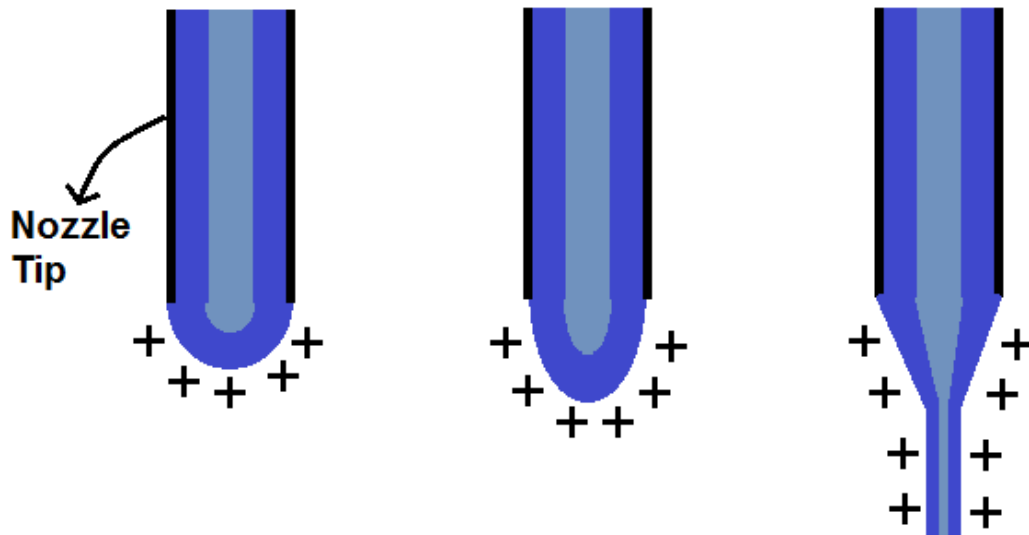


Figure 2.4. Taylor cone formation in coaxial electrospinning (modified from the reference [13])

2.4.2. Coaxially Electrospun Nanofibers for Drug Delivery Applications

Core and shell structure of the fibers provides a great potential to synthesize a single product with unique properties that are difficult to obtain from separate electrospinning of the same materials. It is similar to blending of materials but different from it as the two materials maintain their separate features. It can also be seen as a one-step method for obtaining a coated product.

Production of core-shell nanofibers via electrospinning may be considered as a revolutionary development for biomedical applications. Many studies were performed where core shell nanofibers were produced involving variety of materials with novel structures for new applications. By using those materials, sustained delivery of the drugs can be achieved with core-shell structured fibers as carriers [52].

The biomedical applications of core-shell nanofibers besides controlled drug release are [53-55]:

1. Isolation of an unstable component for protecting it from decomposition under a highly reactive environment.
2. Reinforcement of a material for improving its mechanical properties.
3. Scaffold production for tissue engineering where a less biocompatible polymer is surrounded by a biocompatible one.

In addition to controlled release of drugs, coaxially electrospun nanofibers can also be used for one-step encapsulation and controlled release of plasmid DNA, peptides and growth factors and other biomolecules which are involved in tissue regeneration. The process eliminates the damages caused by direct contact of the agents with harsh conditions or organic solvents. The shell layer acts as a barrier by preventing the burst release of the molecules inside the core. Release of the encapsulated agents is modulated by varying the composition and structure of the nanofibers.

In one of the related studies performed by Huang et al., the release profile of two drugs (resveratrol and gentamycin sulfate) were investigated. PCL was used as the shell solution and two drugs (gentamycin sulfate in water and resveratrol in ethanol) were used as the core solutions. Drug release profiles of the coaxially electrospun products was in a sustained manner without the burst release [56]. Another research performed by Jiang et al. found that the lysozyme released from coaxially electrospun core/shell fibers is bioactive and could maintain its structure [57]. The release profile of proteins were further modified by adding PEG to the shell solution. As the flow rate of the core solution increased, the loading efficiency and release rate of proteins increased, too [58]. Moreover, Saraf et al. was able to achieve non-viral gene delivery with coaxial electrospinning [59] and Liao et al. used coaxial electrospinning for sustained viral gene delivery. These are some of the promising

works that was done with coaxially electrospun nanofibers which can be used in local drug delivery, tissue engineering and wound healing applications [60].

2.4.3. Modified Coaxial Electrospinning

Coaxial electrospinning was previously done with both fluids being electrospinnable or at least the shell fluid was preferred to be electrospinnable [51, 58, 61]. Modified coaxial electrospinning is a recently developed technique where an unspinnable shell solution and a spinnable core solution are used. Previously, a modified process based on coaxial electrospinning was done. In this process only the organic solvents were used as shell fluid. In that study, the modified process was mainly used to manipulate the diameters of the nanofibers. It was found that with a mixture of solvents as the shell fluid, the nanofiber quality can be improved effectively. The improved features include fiber size, size distribution, fiber textures and surface smoothness [62]. This process was also used for production of poly-acrylonitrile nanofibers as carbon nanofiber precursors where again unelectrospinnable solutions were used as shell fluids [63-65].

After verifying that unspinnable solvents can be used as shell fluids, dilute polymer solutions were also used as shell fluids. This type of coaxial electrospinning was particularly used for controlled release studies for production of zero-order drug release membranes. In one research, an unspinnable dilute zein solution was used as shell fluid and an electrospinnable zein/ketoprofen mixture was used as the core fluid. In another study, ketoprofen (KET) was chosen as a model hydrophobic drug and cellulose acetate was used in the dilute shell solution and in the core solution as a mixture with KET. In both studies, the chosen drug (Ketoprofen) was found to have a good compatibility with the polymers. Moreover, it was easily dissolved in the organic solvents and was fully mixed with the polymers inside the core solution. These two features helped to eliminate the burst release in addition to the main effect of the shell layer of nanofibers [19, 20].

In this research, modified coaxial electrosinning was used for controlled release of a hydrophilic drug (ampicillin), which is known to have a low compatibility with the polymer (polycaprolactone). Moreover, a partially electrospinnable shell solution (4% w:v PCL), was used instead of a fully unspinnable one.

2.5. Characterization Techniques

The characterization techniques used in this research are scanning electron microscopy, optical microscopy, Fourier transform infrared spectroscopy and UV-Vis spectroscopy.

2.5.1. Scanning Electron Microscopy (SEM)

Scanning electron microscope (SEM) is the type of electron microscope, which uses a focused beam of electrons for the production of sample images with high magnification. The electrons of the microscope interact with atoms on the sample surface. As a result, various signals are produced and they are detected. The surface topography of the sample is analyzed with the help of those signals. The resolution of SEM can be as low as 1 nanometer. The lenses of SEM (condenser and objective lenses) are used for focusing the electron beam to a particular spot.

2.5.2. Optical Microscopy

Optical microscope (also called light microscope) magnifies the image of the sample by using visible light and a set of lenses. It consists of ocular lenses, objective lenses, light source, focus knobs (for fine adjustment and coarse adjustment), stage, diaphragm-condenser and finally the mechanical stage. The magnification of an optical microscope is the product of the powers of the ocular and the objective lens. Focus knobs are for moving the stage in order to focus on the image. A condenser

and diaphragm are used to concentrate light from its source so that it is focused onto the sample.

2.5.3. Fourier Transform Infrared Spectroscopy (FTIR)

Fourier transform infrared spectroscopy (FTIR) spectrometer is able to collect high spectral resolution data for a wide spectral range. It shines a beam of light with many frequencies at once in order to measure the absorption of the beam by the sample. The beam with different combinations of frequencies is given many times and the absorptions of different wavelengths are inferred by the computer.

2.5.4. Ultraviolet–visible spectroscopy (UV-Vis Spectroscopy)

Electromagnetic radiation (for example visible light) is considered as a wave phenomenon and it is characterized by a wavelength or frequency. The distance between adjacent peaks refers to the wavelength. On the other hand, frequency is the number of wave cycles that pass through a certain point per time. The UV-Vis spectrometer scans all the component wavelengths over a short period time. The visible light region is from 400 to 800 nm and the UV region scanned is from 200 to 400 nm. The absorbance is displayed on the vertical axis and the wavelength is displayed on the horizontal axis. λ_{max} is the wavelength of maximum absorbance and it is a characteristic value of samples.

3. MATERIALS AND METHODS

3.1. Materials

Polycaprolactone (catalog #: 440744, Mw: 80000 DA), PBS tablets (catalog #: P4417), Crystal Violet (catalog #: 61135) and methanol (catalog #: 34885) were obtained from Sigma Aldrich (USA). Chloroform was obtained from Merck (catalog #: 102431). Ampicillin sodium salt (catalog #: A0839) was purchased from AppliChem (USA). Ampicillin is an antimicrobial agent which is a part of penicillin group of beta-lactam antibiotics. It is able to penetrate a broad spectrum of bacteria by inhibiting the enzyme which synthesizes the bacterial cell wall [32]. The molecular weight of PCL was chosen based on its suitability for drug release applications as reported in the literature [66].

3.2. Methods

3.2.1. Optimization Studies for Core and Shell Solutions

A preliminary study was performed prior to the production of drug release membranes in order to determine and optimize certain parameters of production. The investigated parameters were applied voltage, needle tip to collector distance and shell polymer concentration. In the first part, optimization of electrospinning system parameters was carried out. Among five system parameters, needle gauge and collector type was kept constant. Among the remaining parameters optimization of tip to collector distance and the applied voltage was carried out at constant core solution flow rate. For determining these parameters, optimization of the flow rates of core and shell solutions were performed during the synthesis of membranes. In the second part, the concentration of shell solution was determined. For this purpose, the electrospinnability of PCL solutions with different PCL concentrations was tested. Two features were paid attention in this part. One of them is the electrospinnability of the solution and the other one is polymer concentration. Among those properties,

the solution with highest concentration while not being fully electrospinnable was chosen. All experiments were carried out at room conditions.

In this research, the solvent ratios for all electrospinning solutions were kept constant at chloroform:methanol (9:1, by volume) [32].

3.2.1.1. Optimization of Electrospinning Parameters

In this part, applied voltage range and distance between needle tip and the collector were determined by using single electrospinning of the PCL/Ampicillin solution. Those two parameters were kept constant throughout the experiment after being optimized.

For the production of the electrospinning solution, 0.1 gram of ampicillin was dissolved in 0.2 ml of Methanol. On the other hand, 0.5 gram Polycaprolactone was dissolved in a solvent mixture containing 4.5 ml Chloroform and 0.3 ml Methanol for two hours. After both PCL and Ampicillin were dissolved, two solutions were mixed to prepare the final solution containing 10% (weight:volume) PCL and 2% w:v Ampicillin with 9:1 v:v chloroform:methanol as solvent. This solution was mixed for another hour.

Table 3.1. Electrosopinning parameters investigated in the preliminary studies

Preliminary Studies Part 1		Preliminary Studies Part 2
Tip to Collector Distance	Applied Voltage	PCL Concentration
9-10 cm	8-12 kV	3-5 % (w:v)

In the literature, tip to collector distance was kept 8 cm [32]. In this research; the distance was tried to be increased. For that purpose, the distances was varied in the range 8-10 cm by 1 cm increments. After the optimal distance was determined, the voltage values between 8-12 kV were also tested in order to find out the optimal

voltage. The optimization process was carried out by keeping the core solution flow rate 1 ml/h.

3.2.1.2. Electrospinnability of Solutions with Different PCL Concentrations

In this part, PCL solutions with three different PCL concentrations were prepared and their electrospinnability was observed. A total of 0.15, 0.20 and 0.25 grams of PCL were dissolved in 0.5 mL Methanol and 4.5 ml Chloroform for an hour in order to produce 3%, 4% and 5% w:v PCL solutions, respectively. For the electrospinning of the solutions, parameters that were determined at the optimization part were used. The applied voltage was kept 12 kV and the tip to collector distance was kept 9 cm. The flow rate of all the solutions was 1 ml/h.

In order to observe the electrospinnability of the solutions, the samples were collected on microscope slides which were put on the 15x15 cm² Aluminum collector. The samples were observed under optical microscope (Nikon Eclipse, LV100).

On the basis of this data obtained in preliminary observations, the results were evaluated and the optimum process parameters were clarified for further studies.

3.2.2. Coaxial Electrospinning and Production of Membranes

In the experiment, stainless steel co-axial nozzle (Inovenso, Turkey) was used for the formation of core-shell structures. It has two inputs for two different fluids. The input for the shell fluid is on the left and the input for the core fluid is on the top of it. The two fluids are finally united on the bottom tip (Figure 3.1). The inner diameter of the nozzle tip is 0.7 mm and the outer diameter is 1.2 mm (Figure 3.2).

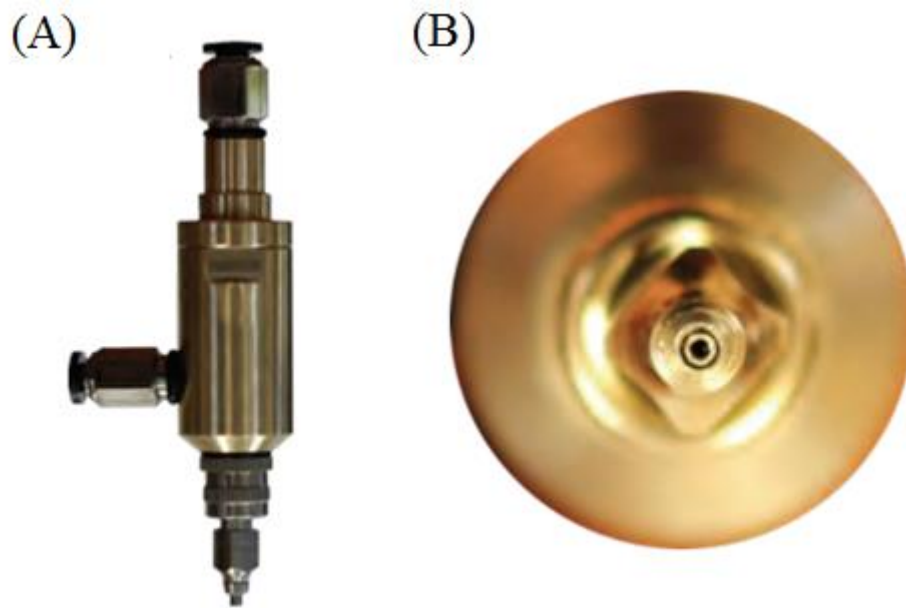


Figure 3.1. Coaxial electrospinning nozzle (A) Side view (B) Bottom view

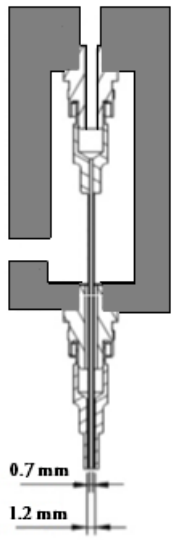


Figure 3.2. Sketch of a coaxial nozzle

Table 3.2. Flow rates and compositions used for production of samples

Fiber Name	Composition		Flow Rate (ml/h)	
	Core Fluid	Shell Fluid	Core	Shell
CS1 (Core/Shell 1)	10 % (w:v) PCL 2% (w:v) ampicillin	4 % (w:v)PCL	0.5	0.5
CS2 (Core/Shell 2)	10 % (w:v) PCL 2% (w:v) ampicillin	4 % (w:v) PCL	0.5	0.6
CR (Core)	10 % (w:v) PCL 2% (w:v) ampicillin	Not Present	1.0	-
Shell	Not Present	4 % (w:v) PCL	-	1.0

Before electrospinning, core and shell solutions were prepared separately. The core solution was a 10% w:v PCL solution containing 2% w:v ampicillin. It was the solution used during the optimization process and its preparation is explained in section 3.2.1.1. The shell solution was a 4% PCL solution, the preparation of which is explained in section 3.2.1.2. The solutions were drawn into syringes.

Two syringes containing core and shell solutions were separately placed into two syringe pumps. The diameter of the syringes was 12.06 mm. For production of CS1 membranes, the core and shell flow rate were both kept at 0.5 ml/h. For production of CS2 membranes, the core flow rate was kept at 0.5 ml/h and the shell flow rate was kept at 0.6 ml/h. For single electrospinning of the core (CR membrane), the shell flow rate was kept at 0 ml/h and core flow rate was kept at 1 ml/h. For single electrospinning of shell solution, the shell flow rate was kept at 1 ml/h and core flow rate was kept at 0 ml/h (Table 3.1).

The distance between nozzle tip and the collector was kept 9 cm and the voltage was kept 12 kV. These parameters were determined by the preliminary work described in section 3.2.1.1. The schematic representation of the process is illustrated in Figure 3.3.

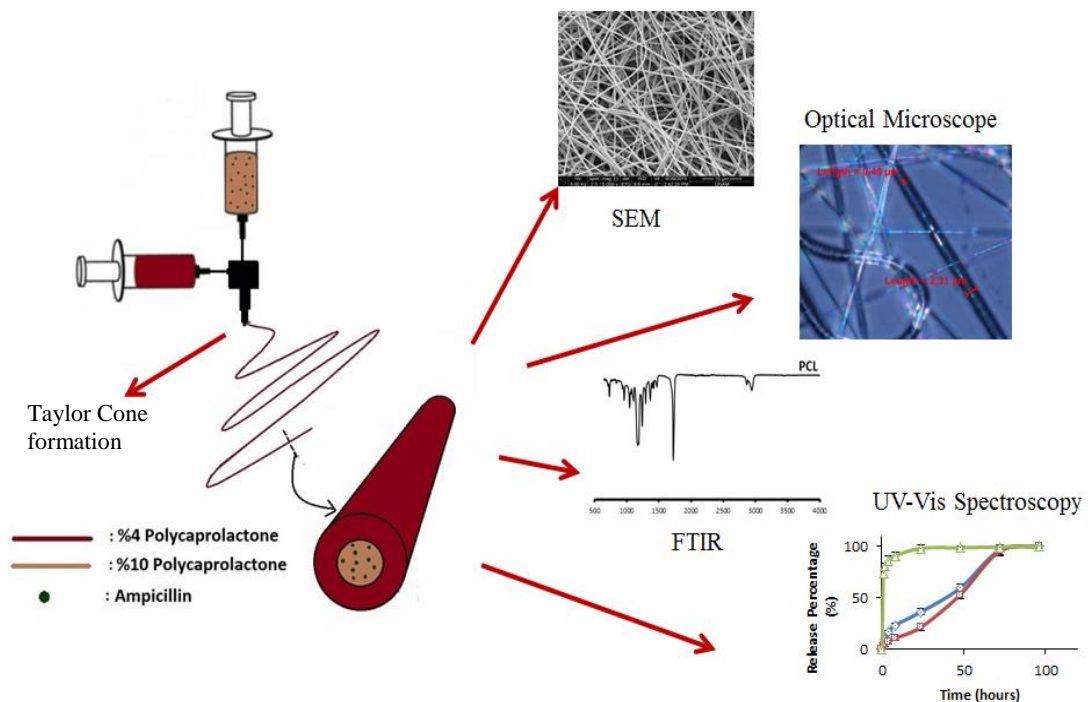


Figure 3.3. Schematic of the process of formation of core-shell nanofibers (modified from reference [67])

For observation of core-shell structure under Optical Microscopy, the process was run for 30-60 seconds. The samples were collected on microscope slides which were attached to the Aluminum collector.

Core solution was stained with Crystal Violet for one time in order to take the photograph of the Taylor cone. In other studies, no dye was used. For other characterization techniques and drug release studies, the electrospinning was carried out for 4 hours and a 15x15 cm² Aluminum foil was used as the collector. Figure 3.4 is a photograph of the system which was used in this study.

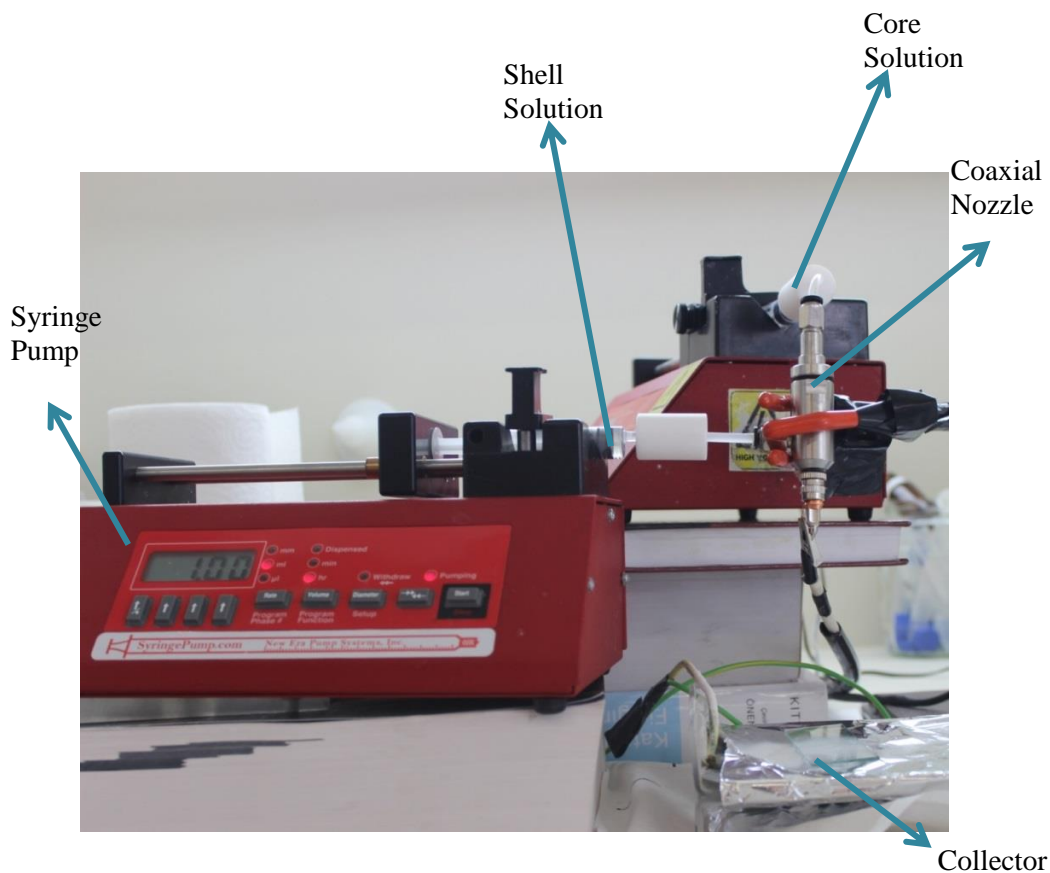


Figure 3.4. Photograph of coaxial electrospinning system used in the study

3.2.3. Characterization of the Membranes

The morphology of the membranes was observed under environmental scanning electron microscope (FEI-Quanta 200 FEG, ABD). Prior to the examination, the samples were sputter-coated with gold. Images with different magnification were taken (2500x, 5000x, 20000x, 50000x)

The average fiber diameter of three different samples was found by measuring their diameters from SEM images at 50 different places for each sample using Image J software (NIH, MD, USA).

The core-shell structures of the nanofibers collected on microscope slides were observed under optical microscope (Nikon Eclipse, LV100).

The compatibility between components of the membranes was investigated by Attenuated total reflectance Fourier transform infrared (ATR-FTIR) analysis. It was performed with a FTIR spectrometer (Perkin Elmer Spectrum, 100, USA) from 650 to 4000 cm^{-1} .

3.2.4. Drug Release Studies

In vitro drug release profile of ampicillin from the electrospun membranes was examined by measuring the ampicillin concentration released into phosphate buffered saline (PBS, pH: 7.4) solution with UV-VIS spectrophotometer (Hitachi U-5100, Japan).

Firstly, in order to measure the ampicillin release profile, maximum absorbance of as purchased ampicillin in PBS was studied and it was found to occur at the wavelength of 325 nm. The absorption of solutions with predetermined drug concentrations was measured in order to draw a calibration curve based on this wavelength. The resulting calibration curve is shown in Figure 3.5. It was later used to calculate the ampicillin concentrations released from the membranes into the PBS solutions.

Secondly, the membranes were kindly separated from the aluminum foil. Then, they were cut to form squares with dimensions of $1.5 \times 1.5 \text{ cm}^2$ which weighed 100 mg on average. They were kept in desiccator overnight to remove any remaining solvent.

A PBS tablet was dissolved in 100 ml of distilled water for preparing the PBS solution (pH: 7.4). A total of 4 ml of PBS was poured into 4 wells of a 12-well plate. The samples were immersed into 3 of the wells, the remaining one was used as negative control. The 12 well plate was placed inside a 37°C orbital shaking bath (MAXQ 4450 Thermoscientific) and the shaking speed was adjusted to be 50 rpm. At certain time intervals (1, 2, 4, 8, 24, 48, 72 and 96 hours) 1 ml of sample solution was taken and replaced with 1 ml of stock PBS solution. The absorption values of all

the sample solutions taken for different time intervals were determined by the UV-VIS spectrophotometer at the wavelength of 325 nm.

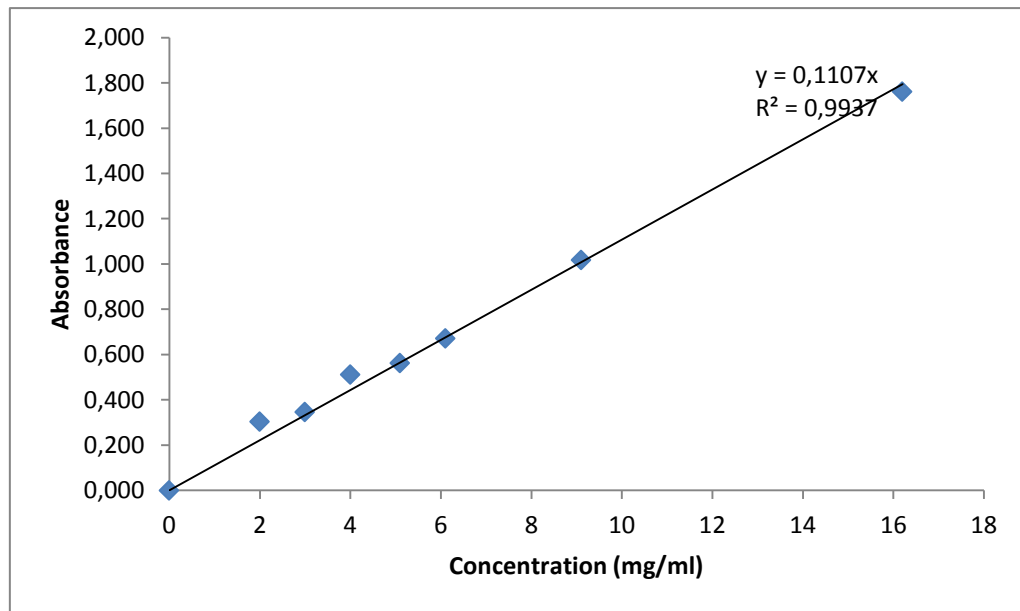


Figure 3.5. Calibration curve for ampicillin concentration in PBS

Finally, the drug encapsulation efficiencies of three membranes were found. 10 mg of each membrane was dissolved in 5 ml chloroform. After they are fully dissolved, 5 ml of PBS was added and the solution was vortexed for 45 minutes. Following the phase separation of chloroform and PBS, the concentration of ampicillin inside the PBS was found with UV-VIS spectrophotometer at the wavelength of 325 nm. Each experiment was repeated three times.

3.2.5. Statistical Analysis

SPSS 22.0 for Windows was used in statistical analysis. The fiber diameters and the drug encapsulation efficiencies of three membrane groups (CR, CS1, CS2) were compared. One-way ANOVA (analysis of variance) test followed by Tukey's HSD (honestly significant difference) test was employed for testing the significance.

Sample size was 50/group for testing fiber diameters and 3 for drug encapsulation efficiency. The data were shown as the mean \pm SD and the p value (significance) for both tests was set as $p < 0.05$.

4. RESULTS AND DISCUSSION

4.1. Results of the Preliminary Studies

In the first part of the preliminary studies, optimization of the electrospinning parameters was carried out. In addition to obtaining a stable Taylor cone, the parameters that result in minimum plugging were also studied. Plugging is the aggregation of the polymer on the needle tip, which causes blocking of the fluid flow. Moreover, increasing tip to collector distance reduces the formation of fused fibers and results with finer fibers. For this purpose, three different distances, 8-10 cm, were tested. For all distances a stable Taylor cone was obtained; however, the minimum plugging was observed for 9 cm tip to collector distance. When the distance was increased to 10 cm, the polymer on the tip blocked the fluid flow a few minutes after initiating the process. However, when the distance was 9 cm, plugging did not occur for a longer period (more than 10 minutes).



Figure 4.1. Photograph of a stable Taylor cone

While keeping the distance 9 cm, different voltage values were tested. When the voltage was below 9 kV, Taylor cone did not occur properly and dropping of the solution was observed. Plugging was observed with all voltages after some time; however, minimum plugging happened when the voltage was 12 kV. When the voltage was above 12 kV, more than one jet was observed. As a result, 9 cm tip to collector distance and 12 kV applied voltage were chosen as working parameters in the next steps. In figure 4.1, a stable Taylor cone without plugging is shown when tip to collector distance was 9 cm, applied voltage was 12 kV and the flow rate was 1 ml/h.

In the second part of the preliminary studies, the electrospinnability of solutions with different PCL concentrations were tested. This was done in order to determine the concentration of shell solution, which will be used in drug release membrane production. Previously it was thought that only a highly electrospinnable shell solution could be used in coaxial electrospinning; however, a modified coaxial electrospinning technique was developed where a dilute unspinnable shell solution can be used. As this modified electrospinning technique was used in this study, a partially unelectrospinnable shell solution was preferred. It is known that, electrospinnability changes with polymer concentration. On the other hand, as the polymer concentration of shell solution increases, the coaxial fibers could be coated with a thicker shell layer. The shell layer was desired to be thick enough to prevent the burst release. For those purposes, a shell solution with highest PCL concentration without being electrospinnable was investigated. The optical images could be a good indicator for the electrospinnability of the solutions. If the image is only formed by micro/nanoparticles, it is understood that the solution was not electrospinnable. The images of fibers/particles produced from 3%, 4% and 5% PCL solutions with 50X magnification can be seen in Figure 4.2, Figure 4.3 and Figure 4.4, respectively.

For the sample prepared from 3% PCL (w:v) solution, it can be seen from the optical microscopy image that only micro/nanoparticles were produced and it was not electrospinnable.

For the sample prepared from 4% (w:v) PCL solution, both micro/nanoparticles and micro/fibers with beads were produced. This sample was also not fully electrospinnable and it was chosen as the shell fluid. In Figure 4.5, another image of this sample with 100x magnification is shown.

For the sample prepared from 5% (w:v) PCL solution, mainly fibers with beads were obtained. As this solution is fully electrospinnable, it was not chosen as the shell fluid.

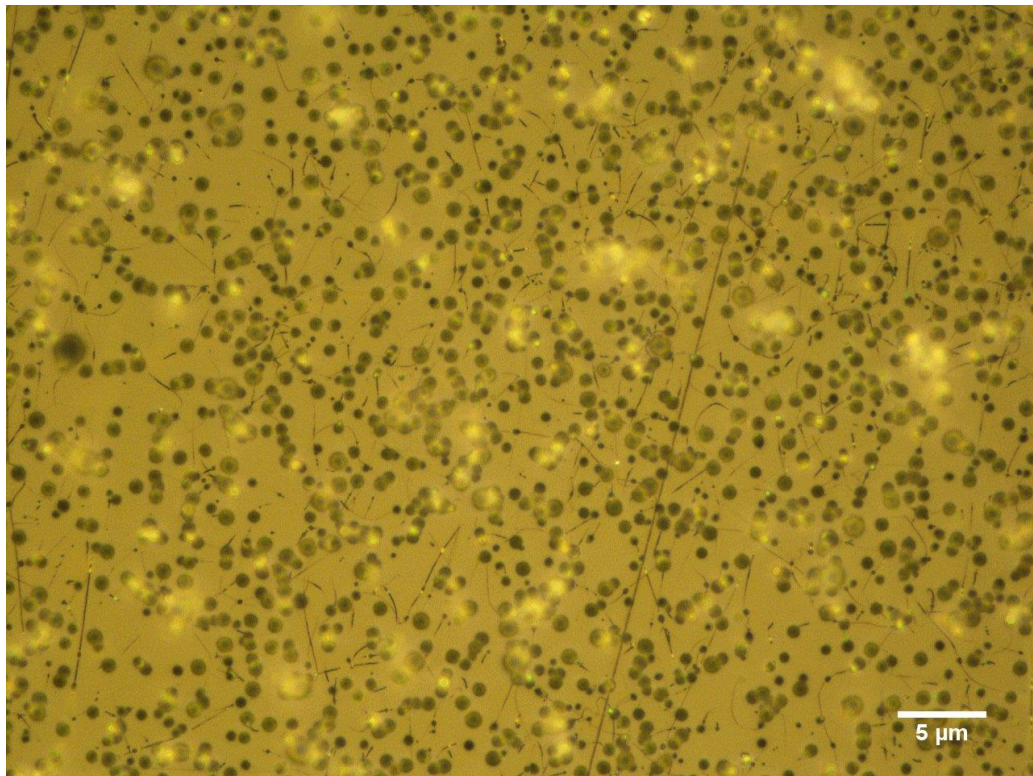


Figure 4.2. Electrospinning product of 3% (w:v) PCL

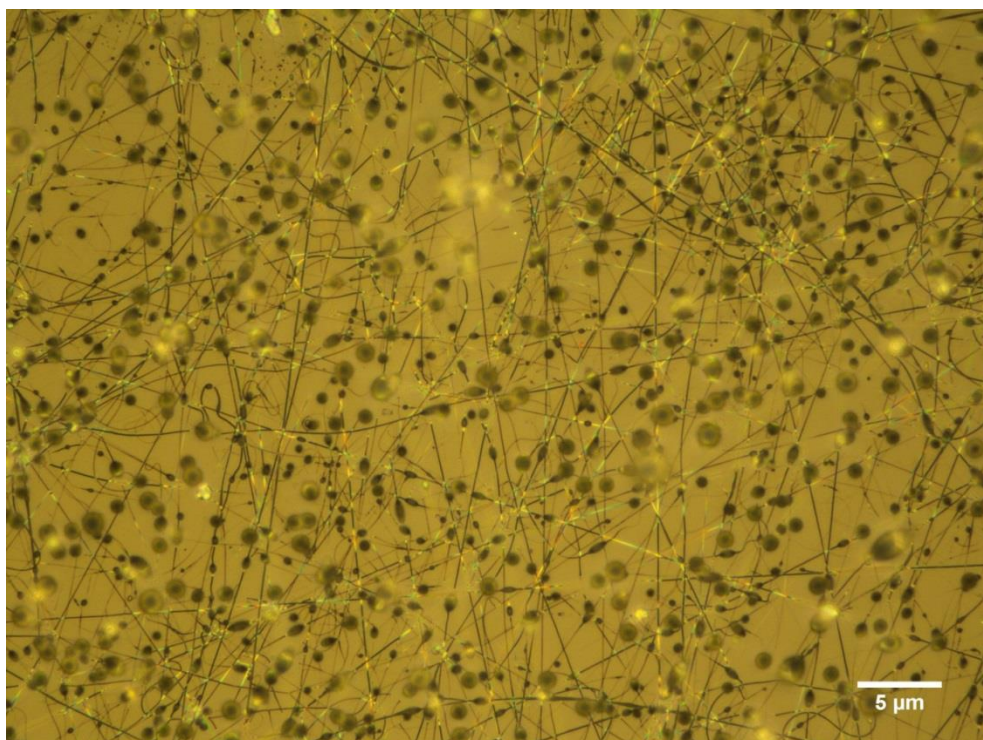


Figure 4.3. Electrospinning product of 4% (w:v) PCL

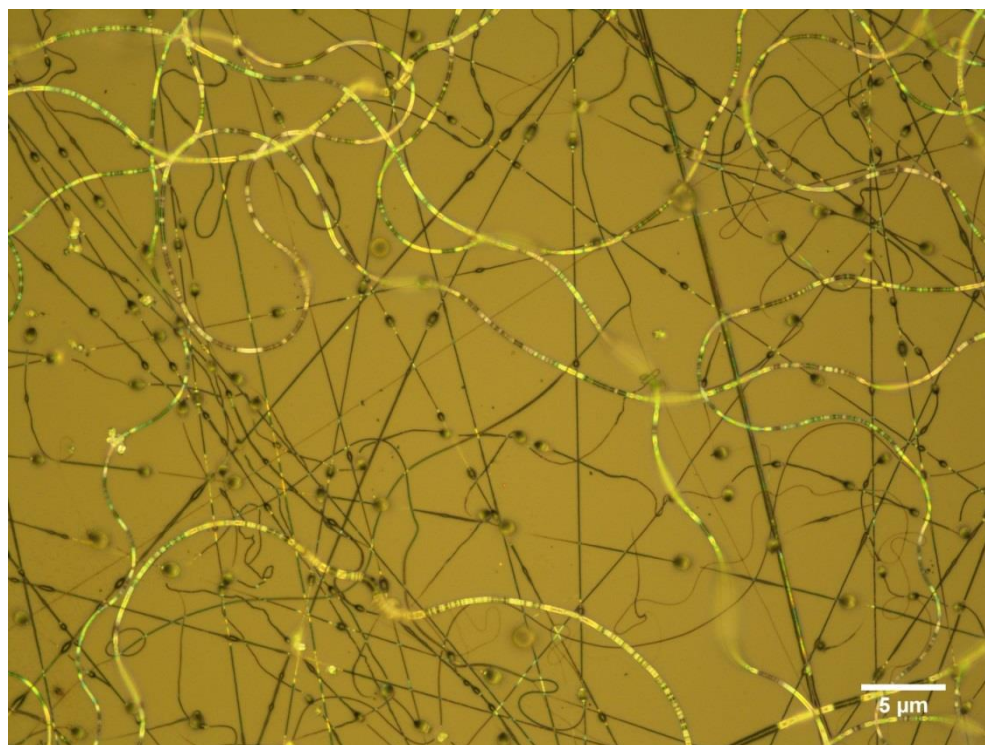


Figure. 4.4. Electrospinning product of 5% (w:v) PCL

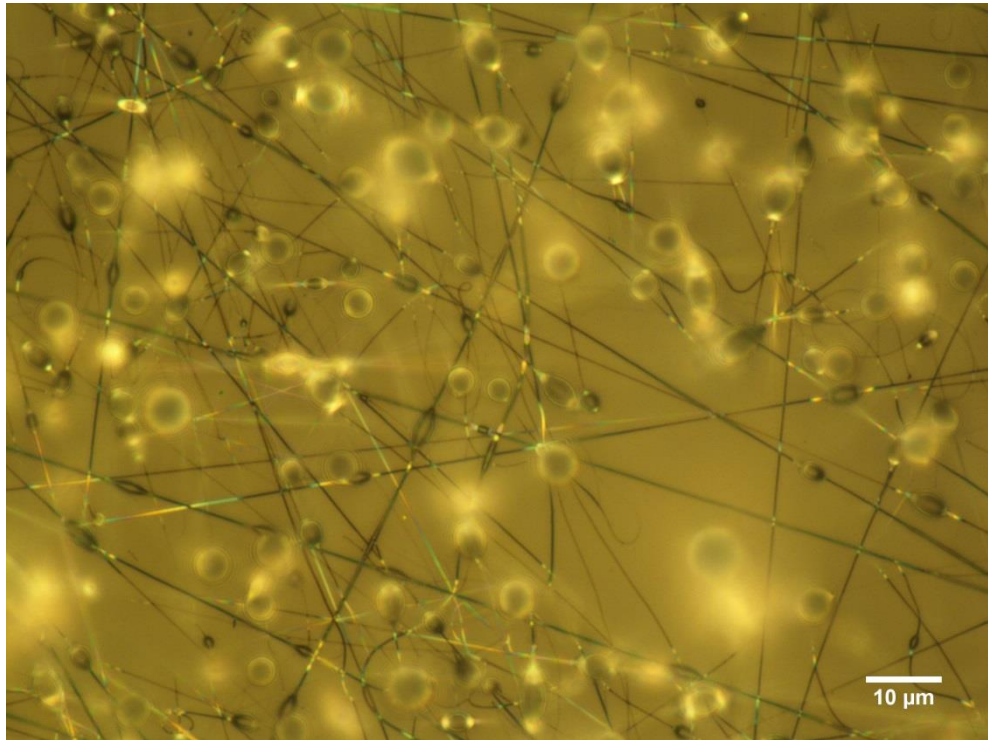


Figure 4.5. Higher magnification of 4% (w:v) PCL electrospinning product

4.2. Taylor Cone Formation in Coaxial Electrospinning

Formation of stable Taylor cone is essential in order to obtain membranes with fine and uniform nanofibers. For this purpose, the optimization process for obtaining a stable Taylor cone was carried out. In this process, effect of the flow rates of core and shell solutions on the formation of stable Taylor cone was investigated. In order to reduce complexity, all the other parameters were kept constant except the flow rates. On the basis of data obtained in preliminary studies, tip to collector distance was kept 9 cm and the voltage was kept 12 kV. The same collector was used for all experiments. (For the experiment where microscope slides were used, the slides were put on that collector.) The flow rate values, which resulted in stable Taylor cone, are listed on Table 4.1.

Table 4.1. Electrospinning parameters used for production of membranes

Sample Name	Composition		Flow Rate		Distance	Applied Voltage
	Core Fluid	Shell Fluid	Core Fluid	Shell Fluid		
CR	10 % (w:v) PCL 2% (w:v) ampicillin	4 % (w:v) PCL	1 ml/h	-	9 cm	12 kV
CS1	10 % (w:v) PCL 2% (w:v) ampicillin	4 % (w:v) PCL	0.5 ml/h	0.5 ml/h	9 cm	12 kV
CS2	10 % (w:v) PCL 2% (w:v) ampicillin	Not Present	0.5 ml/h	0.6 ml/h	9 cm	12 kV

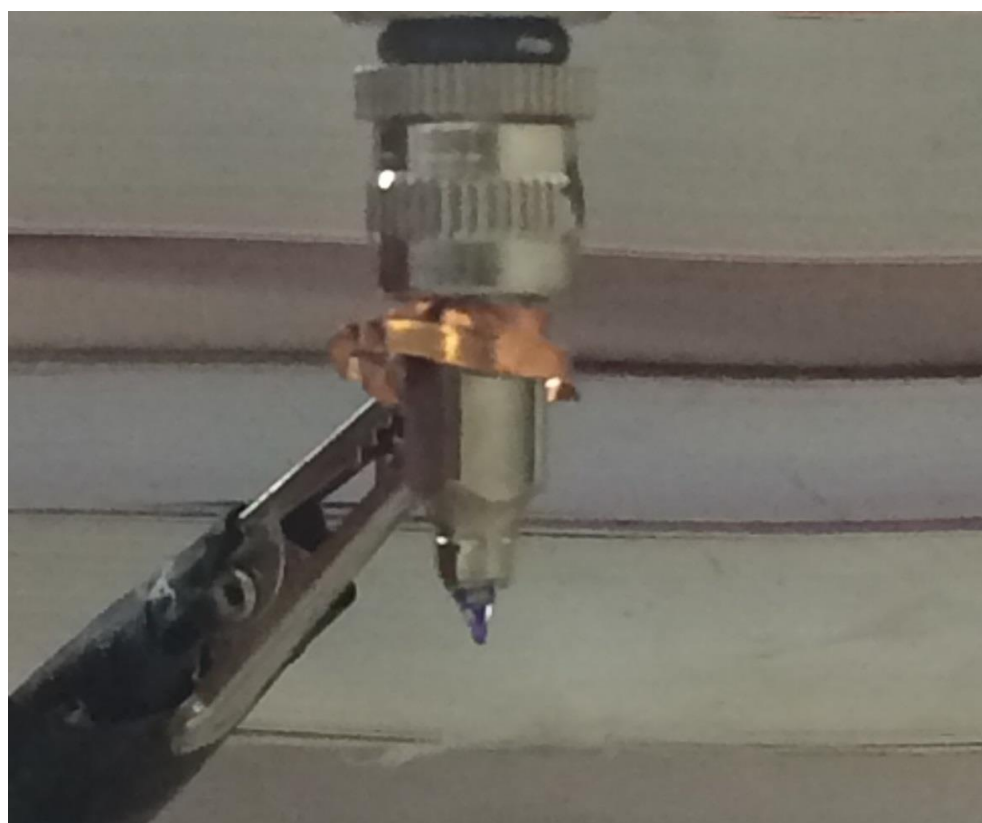


Figure 4.6. Formation of Taylor cone during coaxial electrospinning

For production of core-shell nanofibers, when the shell flow rate was above 0.6 ml/h, the time was not sufficient for solvent evaporation and dropping of the fluid onto the

membranes occurred. This also resulted in destruction of previously formed fibers on the membrane. Moreover, it caused plugging on the needle tip and disturbed the Taylor cone. When the shell flow rate was below 0.5 ml/h, formation of more than one jet was observed on the needle tip. These jets are not desired because core and shell fluids should form a single jet at the end of the Taylor cone for formation of proper core-shell structure. This single jet was observed for the flow rates used to produce the samples, CS1 (Core/Shell 1) and CS2 (Core/Shell 2). The photograph of a stable Taylor cone is shown in Figure 4.6. The core solution was colored by Crystal Violet for showing the core and shell fluids separately on the photograph. It can be seen that the shell fluid successfully covered the core fluid and the Taylor cone formed on the tip of it. Moreover, it was observed that using dilute shell solutions resulted in less plugging on the needle tip. Plugging and blockage of needle tip happened more frequently during the electrospinning of the core alone (production of CR membranes).

The formation of stable Taylor cone was not taken into account while the electrospinning of the shell alone, because it was not used in drug release studies.

4.3. Morphology and Structure of Nanofibers

The SEM images of three sample membranes CR, CS1 and CS2 are shown in Figure 4.8, Figure 4.9 and Figure 4.10, respectively. The morphology of CS1 and CS2 membranes were similar which both had a variation in fiber diameters (less uniform fiber distribution). On the other hand, for the single electrospinning of the core (Sample: CR), more uniform nanofibers were obtained. Nanofibers CR, CS1 and CS2 had average diameters of 702 ± 166 nm, 464 ± 214 nm and 567 ± 180 nm respectively. The p value of ANOVA test was smaller than 0,05 which suggested that one or more pairs of three samples have significantly different fiber diameters. From Tukey's HSD test, all the p values were smaller than 0,05 which demonstrated that the diameters of all three samples were significantly different. The average fiber

diameter of CR was greater than both CS1 and CS2. Moreover, average fiber diameter of CS2 was higher than CS1 (Figure 4.7).

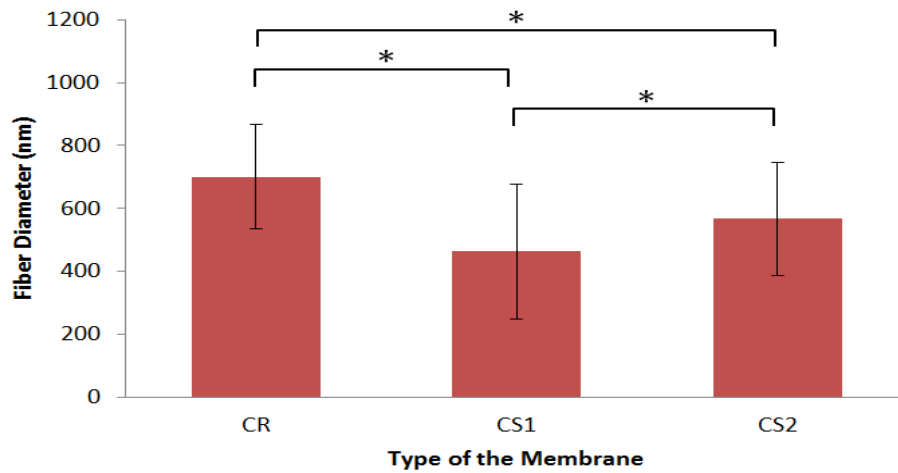


Figure 4.7. Fiber diameters of the membranes (* denotes significant difference at $p < 0.5$)

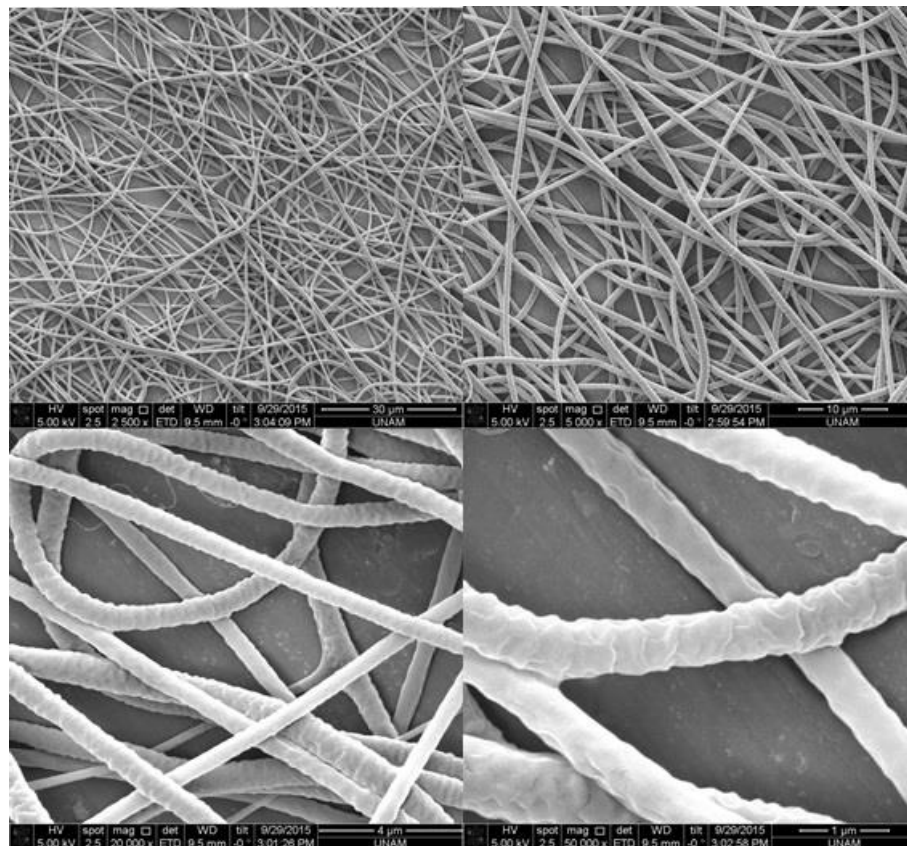


Figure 4.8. SEM image of CR membrane with (a) 2500X, (b) 5000X, (c) 20000X and (d) 50000X magnification

The reason for the difference in fiber diameters is the fact that less solid solutes was exported from the nozzle due to the presence of dilute shell solution in CS1 and CS2. Production of CR membranes was carried out at core flow rate of 1 ml/h, while for production of CS1 and CS2 membranes the core flow rate was 0.5 ml/h. This resulted in less amount of PCL during the electrospinning of core-shell nanofibers. As a result, the fibers produced in this process were finer. When CS1 and CS2 were compared, the reason for CS1 having finer fibers is the fact that CS1 has less solid solutes due to its lower shell flow rate.

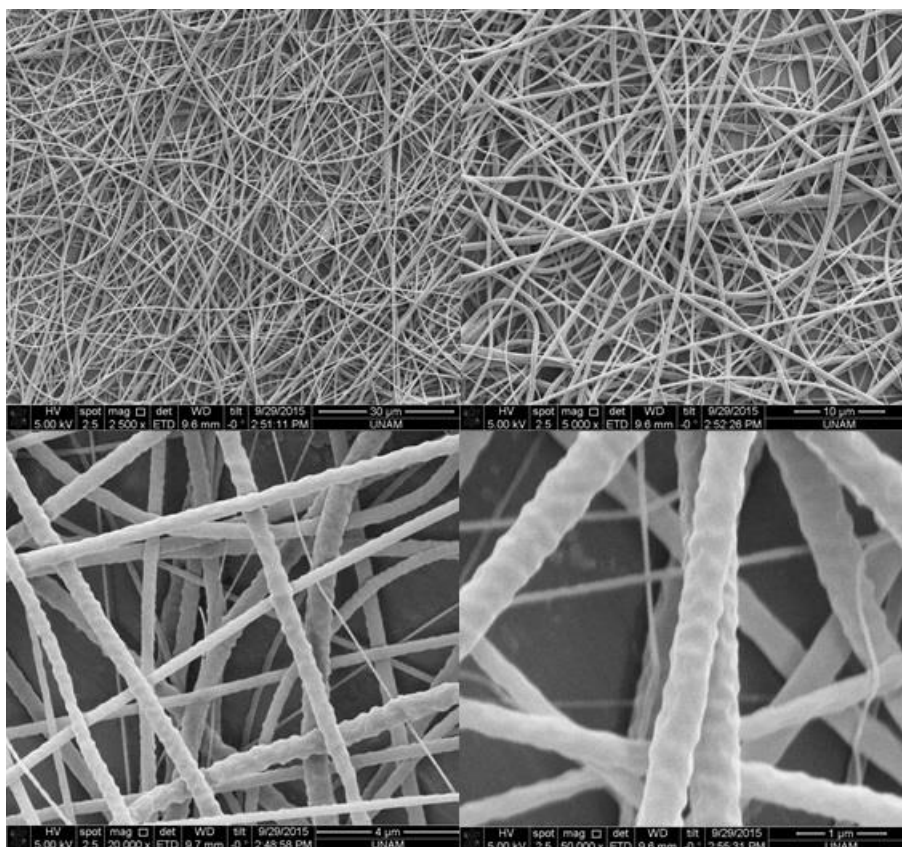


Figure 4.9. SEM image of CS1 membrane with (a) 2500X, (b) 5000X, (c) 20000X and (d) 50000X magnification

In CS1 and CS2 groups, presence of a non-uniform fiber distribution with very fine fibers standing apart from others were observed. For CS1, fibers with diameters even smaller than 100 nm can be seen in Figure 4.9. Those fibers are speculated to be

caused by the extra jets that might be present on Taylor cone. Those jets were especially seen when the flow rate was below 0,5 ml/h but they might have occurred rarely during the production of CS1 and CS2 membranes. It was previously stated that the instabilities during the formation of Taylor cone caused non-uniform fiber distribution and extra jet formation is an example of instability [68]. The low frequency of those fine fibers shows that these problems have happened for a short time and generally the process was successful without extra jet formation.

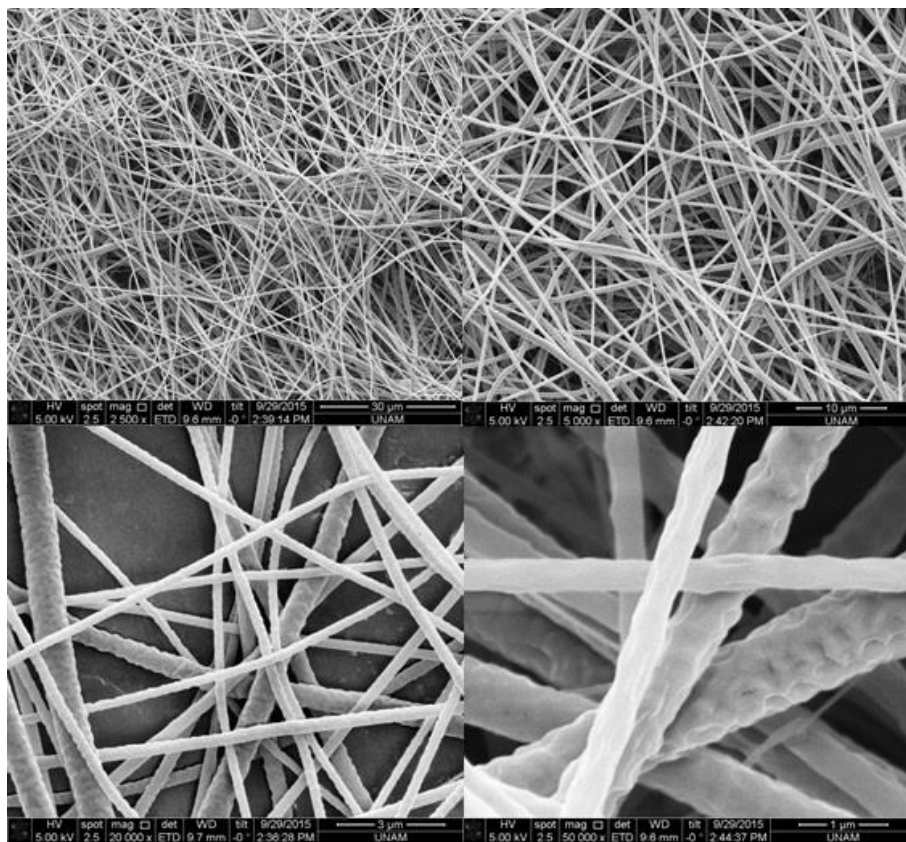


Figure 4.10. SEM image of CS2 membrane with (a) 2500X, (b) 5000X, (c) 20000X and (d) 50000X magnification

Moreover, nanofibers of all the samples had a rough surface morphology. One reason for this can be the low viscosity of the solutions. It was found earlier that fibers become smoother if the viscosity is increased [41]. This might be because of inadequate dissolution of PCL in the solvent mixture due to the low mixing time. It was also found in the literature that the vapor pressure of the solvent affects smooth fiber fabrication. It is stated that rough fiber production is observed when solvents

with low boiling points were used. Both chloroform and methanol used in this research have low boiling points [69, 70].

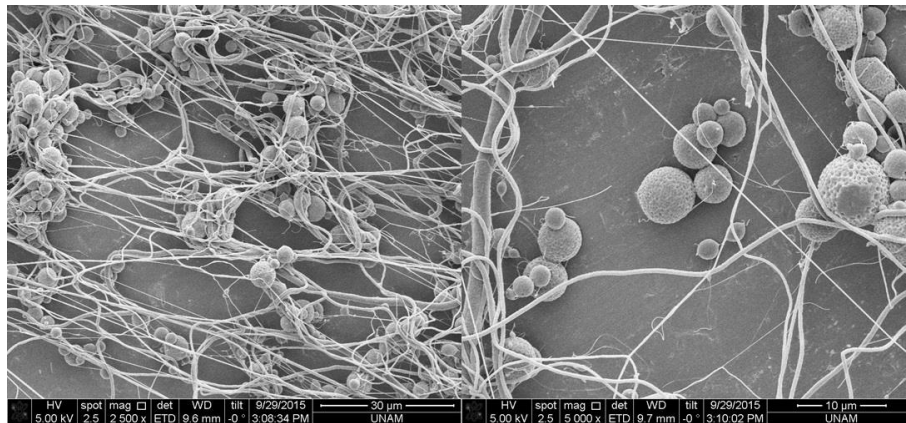


Figure 4.11. SEM image of shell electropinning with (a) 2500X and (b) 5000X magnification

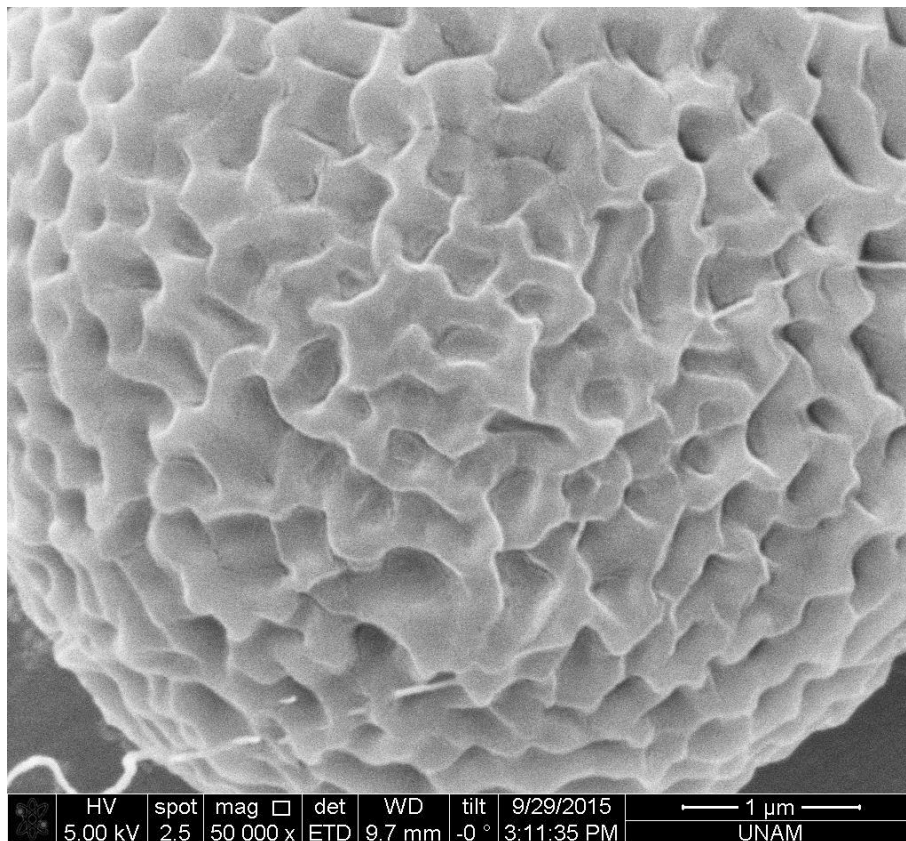


Figure 4.12. SEM image of a microparticle surface produced by shell electropinning

Finally, the morphology of shell solution, which was electrospun alone, was examined (Figure 4.11). Both micro/nanofibers and micro/nanoparticles can be seen in Figure 4.11. On the other hand, no micro or nanoparticle was present on samples CS1 and CS2. The absence of micro/nanoparticles on those membranes proves that shell and core solutions were generally electrospun together while the core-shell structures were being produced. In case of the malfunctioning of the flow regime, a separation of core and shell streams could happen and the electrospinning of them separately should have caused the formation of at least some micro/nanoparticles on CS1 and CS2 membranes.

In Figure 4.12, a 50000X magnification of a microparticle produced by shell electrospinning is shown. The rough surface morphology previously observed on samples CS1, CS2 and CR is present on microparticle surfaces, too. This observation can also be because of low viscosity, low voltage and solvent properties which were the reasons of rough fiber surface of samples CR, CS1 and CS2.

By using optical microscopy the core-shell structure of the fibers were observed. Due to the limitations of optical microscopy, only the fibers with large diameters were examined. The core-shell structure observed for samples CS1 and CS2 are shown in Figure 4.13 and Figure 4.14, respectively. Although, those images do not belong to a typical nanofiber from the samples, they can be seen as indicators for the production of the core-shell structure. In the future, TEM images of the samples will be taken as proofs of core-shell structure.

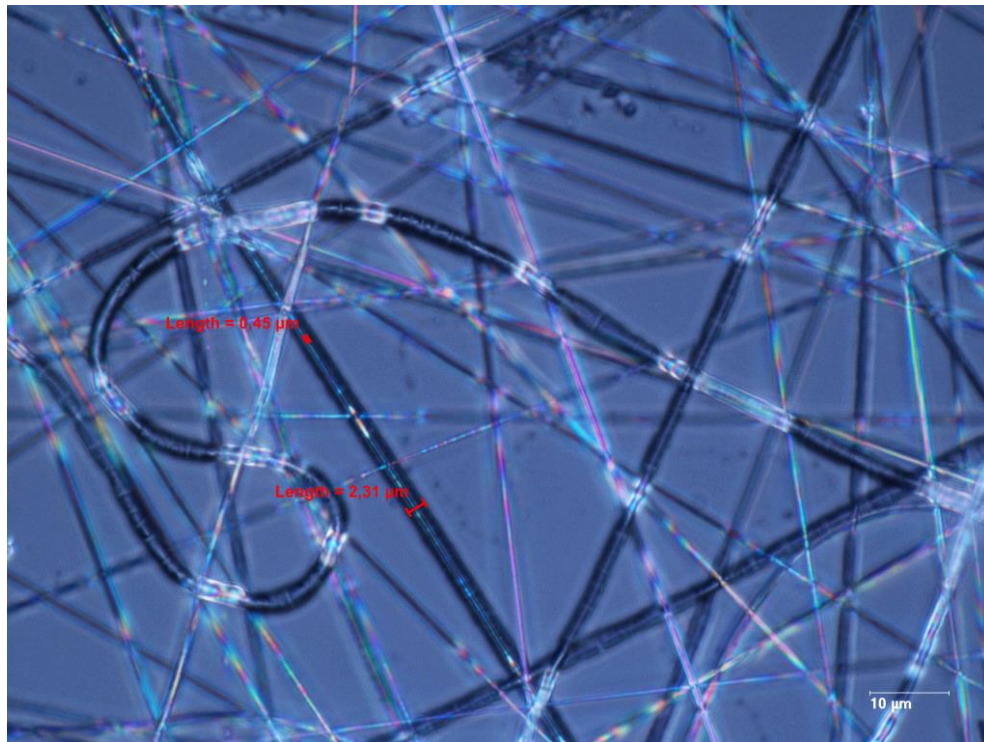


Figure 4.13. Core-shell structure of CS1 membrane



Figure 4.14. Core-shell structure of CS2 membrane

4.4. Compatibility of Components

Compatibility refers to the secondary interactions between the polymer and the drug which slow down the drug release rate. In order to produce a nanofibrous membrane with minimum burst release, compatibility between the components is indispensable. Improvement of compatibility can be achieved via secondary interactions. Hydrophobic interactions, electrostatic interactions and hydrogen bonding are examples of these second order interactions. Hydrogen bonding occurs when a hydrogen atom bound to a highly electronegative atom (fluorine, oxygen or nitrogen) has an attraction to another highly electronegative atom, which is nearby [71]. PCL has oxygen atoms, which can be hydrogen bond acceptors and ampicillin has hydrogen atoms bound to nitrogen, which can be hydrogen bond donors. As a result, hydrogen bonding interactions might be present between PCL and ampicillin inside the nanofibers. The molecular structures of PCL and ampicillin are shown in Figure 4.15.

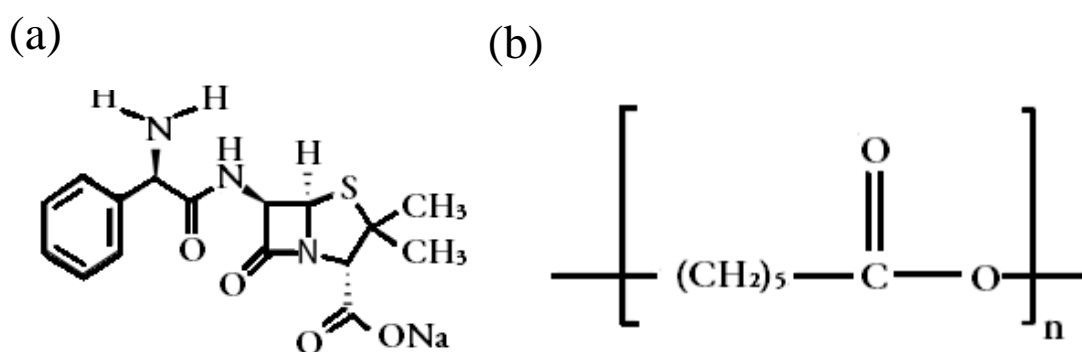


Figure 4.15. Molecular structures of (a) ampicillin and (b) PCL

The ATR-FTIR spectra of the ampicillin, PCL and nanofibers produced from them are shown in Fig. 4.16.

For PCL, several peaks were observed. A strong peak at 1724 shows the C=O stretch which belongs to esters. It can be seen from the spectrum of all samples which include PCL. Such a peak is not present in ampicillin. A medium peak at 2944 shows the C-H stretch which is present in alkanes. A strong peak at 1174 shows the C-O

stretch of esters. A medium peak at 1470 refers to the C–H bends which belongs to the alkanes. A medium peak between 1365 indicates the C–H rock of alkanes.

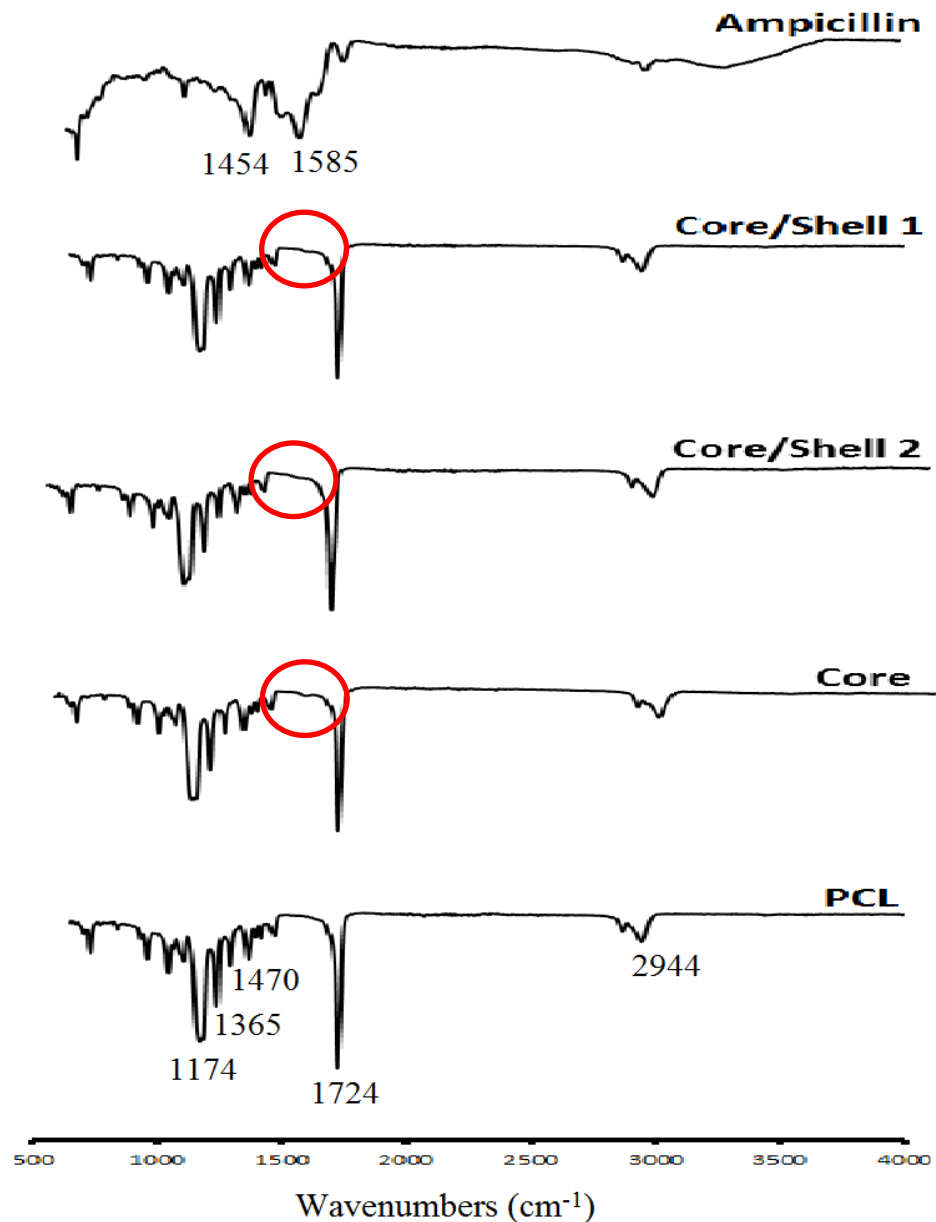


Figure. 4.16. ATR-FTIR spectra of Ampicillin, PCL and electrospun membranes

There are several peaks for ampicillin. The peaks of ampicillin within the range of 650 and 1500 were too close to each other and overlapping was present. Medium peak at 1585 refers to the N–H bend of 1° amines. That peak can also be observed on the FTIR spectra of the membranes (indicated by red circle). This verifies the

presence of ampicillin inside those membranes. Medium peak at 1454 shows the C–C stretch of (in–ring) aromatics. The peak at 1126 indicates C–O stretch. For all the electrospun membranes the peaks generally belonged to PCL because the amount of PCL is much more than ampicillin in these compounds.

4.5. In vitro drug release profiles

Drug release profile was examined with the help of UV spectroscopy by measuring the ampicillin concentration inside the release media between certain time intervals. In order to determine the amount of ampicillin in release media, firstly a calibration curve showing the connection between UV absorbance and concentration in PBS was drawn by using known concentrations of ampicillin. The calibration curve used for this purpose is shown on Materials & Methods section. The formula derived from the calibration curve is:

$$C = 9.033 \times A \quad (4.1)$$

where C is the ampicillin concentration and A is the absorbance of the solution at 325 nm.

It is known from the literature that, in the release environment (PBS), PCL is not swellable and it has a very slow degradation rate [72, 73]. These two features eliminate the swelling controlled and chemically controlled drug release mechanisms. As a result, the controlled release mechanism from PCL membranes is presumed to be diffusion-controlled. Two equations were chosen for describing the diffusion controlled drug release kinetics from sample membranes. Those two equations are Peppas equation (Equation 2.6) and zero-order kinetics equation (Equation 2.3).

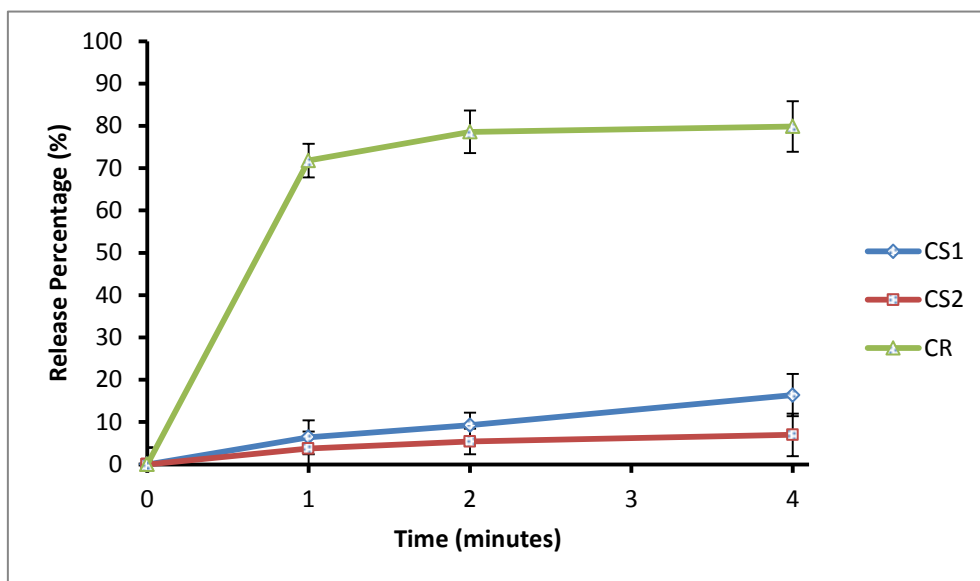


Figure 4.17. In vitro drug release profiles of Core/Shell 1 (CS1), Core/Shell 2 (CS2) and Core (CR) membranes (full range)

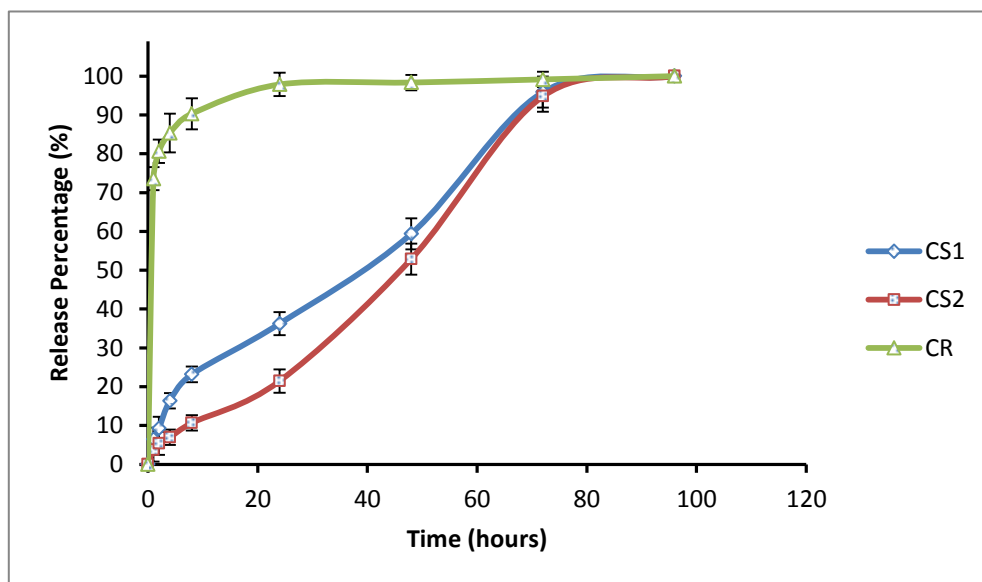


Figure 4.18. In vitro drug release profiles of Core/Shell 1 (CS1), Core/Shell 2 (CS2) and Core (CR) membranes in first 4 hours

The drug release profiles of CS1, CS2 and CR in the first 4 hours are shown in Figure 4.18. The sample named CR produced by single electrospinning of the core

released 85 ± 6 % of the ampicillin within first 4 hours. This indicated the burst release. The coaxially electrospun sample CS1 released 16 ± 2 % of the drug and the one named CS2 released 7 ± 2 % percent of the drug. Both of them have reduced the burst release effect. Moreover, sample CS2, which has greater shell flow rate showed less burst release. This indicates the thickening of shell part of those nanofibers. The burst release observed on sample CR can be due to:

- a) The lower compatibility of ampicillin inside PCL fibers
- b) The accumulation of ampicillin on fiber surface
- c) Absence of a shell layer, which would delay the release

The general drug release profiles of the samples are shown in Figure 4.17. Sample CR released 98 ± 2 % of ampicillin in 24 hours. After the burst release, the lag release period is observed. This release profile can be analyzed by the Peppas equation.

The regressed equation (into Peppas equation) for CR between 0 and 24 hours is as follows:

$$Q_{CR} = 74,885 \times t^{0,0875} \quad (R^2 = 0,9848) \quad (4.2)$$

The k value (74,885) is determined by the structure/geometry of the matrix and the n value (0,0875) represents the release mechanism. The release mechanism can be described as Fickian diffusion when the n value is equal to or below 0,45 [74]. The n value in this equation is much smaller than 0,45 which can be due to the rapid burst release. If the burst release was slower, the n value would be closer to 0,45. Moreover, in a study where release kinetics of metronidazole benzoate from PCL nanofibers was investigated, n values between 0.31-0.44 were found for different drug concentrations. In the same study, it was observed that n value decreased with increase in drug concentration [75]. As a result, another reason for low n value found in this study can be high concentration of ampicillin inside PCL membranes. From

the regression of the formula it can be understood that the drug release from CR membrane was through Fickian diffusion.

Samples CS1 released 96 ± 4 % and CS2 released 95 ± 4 % of the drug within 72 hours. After that, they both entered the lag period. The drug release kinetics of those samples is closer to the zero-order kinetics equation. Peppas equation cannot be applied to those samples due to the non-homogenous distribution of the drug inside the matrix (one of the assumptions of Peppas equation). It was eliminated by the shell layer with blank PCL (without drug).

The regressed equations (into zero order kinetics equation) for CS1 and CS2 between 0 and 72 hours are as follows:

$$Q_{CS1} = 6,9471 + 1,2018t \quad (R^2 = 0,9796) \quad (4.3)$$

$$Q_{CS2} = 0,1341 + 1,2279t \quad (R^2 = 0,9789) \quad (4.4)$$

Q_0 (6,9471 for CS1 and 0,1341 for CS2) refers to the initial amount of drug inside the medium. It should be equal to zero as the release medium has no drug at $t=0$. As the Q_0 value for CS2 membranes is much closer to zero, it is more suitable for zero order kinetics equation. On the other hand, the zero order release constants (1,2018 for CS1 and 1,2279 for CS2) were close to each other with a small difference due to the different shell thicknesses of the membranes. In other studies, where modified coaxial electrospinning was used, the release profile changed with polymer type. When zein was used as the carrier polymer, a release profile closer to zero order release kinetics was achieved in the first 16 hours [19]. Another study found that cellulose acetate was used, a similar release profile was obtained in the first 96 hours [20]. In this study, as the polymer type, the drug, polymer concentration and flow rates are different; a zero order release profile was obtained for the first 72 hours. The release profile can be further changed by changing those parameters for obtaining a profile with less burst release. In another study, a longer release period of a drug (dipyridamole) was achieved by using PCL as the shell layer. However, the

drug release profile was not suitable for zero-order drug release kinetics equation. Moreover, the drug used in that study was a platelet aggregation inhibitor which can be used for dilating the blood vessels in people with several diseases [76]. The desired drug release duration of that process is higher than the one where antibiotics are used. Antibiotics are generally used in wound healing applications where a release duration of even several hours might be sufficient [77].

Moreover, CS2 with higher shell flow rate showed a slower drug release profile than CS1. This shows that the main feature determining the release profile is the shell thickness. The shell thickness can be adjusted by shell flow rate or the polymer concentration of the shell fluid. In section 4.2 it was observed that the shell flow rate can only be between a certain range (0.5-0.6 ml/h) for the formation of stable Taylor cone. Because of this fact, by increasing or decreasing the polymer concentration, the drug release can be easily controlled instead of changing the shell flow rate in future studies.

Finally, the encapsulation efficiencies of three sample membranes were calculated. It was found that the encapsulation efficiencies of CR, CS1 and CS2 are 83.6 ± 1.01 , 93.5 ± 0.54 and 94.7 ± 1.0 , respectively. From the results of the ANOVA test followed by the Tukey's HSD test, it was found that there is no significant difference between the encapsulation efficiencies of CS1 and CS2 ($p > 0.05$). However, CR membrane was significantly different from both CS1 and CS2. The reason of the core shell membranes having higher encapsulation efficiency than the CR membrane is speculated to be due the shell layer. Shell layer of the core shell membranes might have prevented the loss of drug during the membrane production process.

5. CONCLUSION AND FUTURE STUDIES

In this study, ampicillin-loaded PCL nanofibers coated with blank PCL was successfully produced via modified coaxial electrospinning process using dilute and partially electrospinnable PCL solution as the shell. Using 4% (w:v) PCL solution as the shell fluid resulted with less plugging on the needle tip, smaller fiber diameters and sustained release of the drug.

From the SEM images the average fiber diameters were measured as 464 ± 214 and 567 ± 180 nm for shell to core flow rate ratios of 1 (CS1) and 1.2 (CS2), respectively. It was found that average fiber diameter of CR (702 ± 166 nm) was greater than both CS1 and CS2. The reason for the difference in average fiber diameters was thought to be due to the amount of solid solutes exported from the nozzle. The optical images of two core-shell nanofibers from each sample proved that the core was successfully covered with the shell layer. It was demonstrated from the ATR-FTIR spectra that PCL might have some compatibility with ampicillin because of hydrogen bonding. Moreover, presence of ampicillin in the synthesized membranes was verified by the peak which belongs to N–H bend of 1° amines.

Drug release studies showed that nanofibers coated with 4% (w:v) PCL showed a decrease in burst release and a profile closer to linear release was achieved in the first 72 hours due to the shell layer acting as a diffusion-retarding barrier. On the other hand, burst release was observed for single electrospinning of the core solution. Finally, encapsulation efficiency results showed that nanofibers synthesized by coaxial electrospinning have significantly higher encapsulation efficiency than the membranes synthesized by single electrospinning.

In this study, the application area of modified coaxial electrospinning process was extended by using it for the controlled release of a hydrophilic drug. In addition to providing sustained release, the process also resulted with smaller fiber diameters and less plugging compared to single electrospinning. In the future, Transmission

Electron Microscopy images of the core-shell structured nanofibers will be taken. Moreover, the effect of membrane thickness on drug release profile will be examined.

This approach will be used by our research group for further applications which are:

- Additional controlling of the drug release profile by changing the concentration and flow rate of the shell fluid.
- Controlled release of biological agents other than hydrophobic or hydrophilic drugs. Some examples for those agents are peptides, proteins, growth factors and plasmid DNA.
- Production of finer fibers by using the solvent mixture alone as the shell fluid in order to increase the surface area for biosensor applications.

REFERENCES

- [1] Reneker, D. H., Chun, I., Nanometre diameter fibres of polymer, produced by electrospinning. *Nanotechnology*, 7(3), 216, 1996.
- [2] Rodoplu, D., Mutlu, M., Effects of electrospinning setup and process parameters on nanofiber morphology intended for the modification of quartz crystal microbalance surfaces. *J. Eng. Fiber. Fabr*, 2, 118-23, 2012.
- [3] Barhate, R. S., Ramakrishna, S., Nanofibrous filtering media: Filtration problems and solutions from tiny materials. *Journal of Membrane Science*, 296(1-2), 1-8, 2007.
- [4] Manickam, S. S., McCutcheon, J. R., Characterization of polymeric nonwovens using porosimetry, porometry and X-ray computed tomography. *Journal of Membrane Science*, 407, 108-115, 2012.
- [5] Bui, N. N., Lind, M. L., Hoek, E. M. V., McCutcheon, J. R., Electrospun nanofiber supported thin film composite membranes for engineered osmosis. *Journal of Membrane Science*, 385(1-2), 10-19, 2011.
- [6] Kaur, S., Rana, D., Matsuura, T., Sundarrajan, S., Ramakrishna, S., Preparation and characterization of surface modified electrospun membranes for higher filtration flux. *Journal of Membrane Science*, 390, 235-242, 2012.
- [7] Kaur, S., Sundarrajan, S., Rana, D., Matsuura, T., Ramakrishna, S., Influence of electrospun fiber size on the separation efficiency of thin film nanofiltration composite membrane. *Journal of Membrane Science*, 392, 101-111, 2012.
- [8] Nagy, Z. K., Balogh, A., Vajna, B., Farkas, A., Patyi, G., Kramarics, A., Marosi, G., Comparison of electrospun and extruded soluplus (R)-based solid dosage forms of improved dissolution. *Journal of Pharmaceutical Sciences*, 101(1), 322-332, 2012.
- [9] Nagy, Z. K., Nyul, K., Wagner, I., Molnar, K., Marosi, G., Electrospun water soluble polymer mat for ultrafast release of Donepezil HCl. *Express Polymer Letters*, 4(12), 763-772, 2010.
- [10] Yu, D. G., Shen, X. X., Branford-White, C., White, K., Zhu, L. M., Bligh, S. W. A., Oral fast-dissolving drug delivery membranes prepared from electrospun polyvinylpyrrolidone ultrafine fibers. *Nanotechnology*, 20(5), 2009.
- [11] Xiang, A. S., McHugh, A. J., Quantifying sustained release kinetics from a polymer matrix including burst effects. *Journal of Membrane Science*, 371(1-2), 211-218, 2011.

- [12] Chunder, A., Sarkar, S., Yu, Y. B., Zhai, L., Fabrication of ultrathin polyelectrolyte fibers and their controlled release properties. *Colloids and Surfaces B-Biointerfaces*, 58(2), 172-179, 2007.
- [13] Moghe, A. K., Gupta, B. S., Co-axial electrospinning for nanofiber structures: Preparation and applications. *Polymer Reviews*, 48(2), 353-377, 2008.
- [14] Taepaiboon, P., Rungsardthong, U., Supaphol, P., Effect of cross-linking on properties and release characteristics of sodium salicylate-loaded electrospun poly(vinyl alcohol) fibre mats. *Nanotechnology*, 18(17), 2007.
- [15] Wang, X. F., Um, I. C., Fang, D. F., Okamoto, A., Hsiao, B. S., Chu, B., Formation of water-resistant hyaluronic acid nanofibers by blowing-assisted electrospinning and non-toxic post treatments. *Polymer*, 46(13), 4853-4867, 2005.
- [16] Wu, X. M., Branford-White, C. J., Yu, D. G., Chatterton, N. P., Zhu, L. M., Preparation of core-shell PAN nanofibers encapsulated alpha-tocopherol acetate and ascorbic acid 2-phosphate for photoprotection. *Colloids and Surfaces B-Biointerfaces*, 82(1), 247-252, 2011.
- [17] Yu, D. G., Branford-White, C. J., Chatterton, N. P., White, K., Zhu, L. M., Shen, X. X., Nie, W., Electrospinning of Concentrated Polymer Solutions. *Macromolecules*, 43(24), 10743-10746, 2010.
- [18] Yu, D. G., Zhu, L. M., Bligh, S. W. A., Branford-White, C., White, K. N., Coaxial electrospinning with organic solvent for controlling the size of self-assembled nanoparticles. *Chemical Communications*, 47(4), 1216-1218, 2011.
- [19] Yu, D. G., Chian, W., Wang, X., Li, X. Y., Li, Y., Liao, Y. Z., Linear drug release membrane prepared by a modified coaxial electrospinning process. *Journal of Membrane Science*, 428, 150-156, 2013.
- [20] Yu, D. G., Li, X. Y., Wang, X., Chian, W., Liao, Y. Z., Li, Y., Zero-order drug release cellulose acetate nanofibers prepared using coaxial electrospinning. *Cellulose*, 20(1), 379-389, 2013.
- [21] Liu, J. B., Xiao, Y. H., Allen, C., Polymer-drug compatibility: A guide to the development of delivery systems for the anticancer agent, Ellipticine. *Journal of Pharmaceutical Sciences*, 93(1), 132-143, 2004.
- [22] Lodish, H. F., Berk, A., Zipursky, S. L., Matsudaira, P., Baltimore, D., Darnell, J., *Molecular cell biology*. Vol. 4. 2000: Citeseer.
- [23] Lodish, H., Berk, A., Zipursky, S. L., Matsudaira, P., Baltimore, D., Darnell, J., *Noncovalent bonds*. 2000.

- [24] Uhrich, K. E., Cannizzaro, S. M., Langer, R. S., Shakesheff, K. M., Polymeric systems for controlled drug release. *Chemical Reviews*, 99(11), 3181-3198, 1999.
- [25] Kretlow, J. D., Klouda, L., Mikos, A. G., Injectable matrices and scaffolds for drug delivery in tissue engineering. *Advanced Drug Delivery Reviews*, 59(4-5), 263-273, 2007.
- [26] Siepmann, J., Siegel, R. A., Rathbone, M. J., *Fundamentals and applications of controlled release drug delivery*. 2011: Springer Science & Business Media.
- [27] Lin, C. C., Metters, A. T., Hydrogels in controlled release formulations: Network design and mathematical modeling. *Advanced Drug Delivery Reviews*, 58(12-13), 1379-1408, 2006.
- [28] Singhvi, G., Singh, M., Review: in-vitro drug release characterization models. *Int J Pharm Stud Res*, 2(1), 77-84, 2011.
- [29] Costa, P., Lobo, J. M. S., Modeling and comparison of dissolution profiles. *European journal of pharmaceutical sciences*, 13(2), 123-133, 2001.
- [30] Dash, S., Murthy, P. N., Nath, L., Chowdhury, P., Kinetic modeling on drug release from controlled drug delivery systems. *Acta Pol Pharm*, 67(3), 217-23, 2010.
- [31] Streubel, A., Siepmann, J., Peppas, N., Bodmeier, R., Bimodal drug release achieved with multi-layer matrix tablets: transport mechanisms and device design. *Journal of Controlled Release*, 69(3), 455-468, 2000.
- [32] Liu, H., Leonas, K. K., Zhao, Y. P., Antimicrobial Properties and Release Profile of Ampicillin from Electrospun Poly(epsilon-caprolactone) Nanofiber Yarns. *Journal of Engineered Fibers and Fabrics*, 5(4), 10-19, 2010.
- [33] Sill, T. J., von Recum, H. A., Electro spinning: Applications in drug delivery and tissue engineering. *Biomaterials*, 29(13), 1989-2006, 2008.
- [34] Sill, T. J., von Recum, H. A., Electrospinning: applications in drug delivery and tissue engineering. *Biomaterials*, 29(13), 1989-2006, 2008.
- [35] Deitzel, J. M., Kleinmeyer, J., Harris, D., Tan, N. C. B., The effect of processing variables on the morphology of electrospun nanofibers and textiles. *Polymer*, 42(1), 261-272, 2001.
- [36] Thompson, C. J., Chase, G. G., Yarin, A. L., Reneker, D. H., Effects of parameters on nanofiber diameter determined from electrospinning model. *Polymer*, 48(23), 6913-6922, 2007.

- [37] Tan, S., Inai, R., Kotaki, M., Ramakrishna, S., Systematic parameter study for ultra-fine fiber fabrication via electrospinning process. *Polymer*, 46(16), 6128-6134, 2005.
- [38] Kumar, P., Effect of collector on electrospinning to fabricate aligned nano fiber. 2012.
- [39] Koski, A., Yim, K., Shivkumar, S., Effect of molecular weight on fibrous PVA produced by electrospinning. *Materials Letters*, 58(3-4), 493-497, 2004.
- [40] Theron, S. A., Zussman, E., Yarin, A. L., Experimental investigation of the governing parameters in the electrospinning of polymer solutions. *Polymer*, 45(6), 2017-2030, 2004.
- [41] Li, Z., Wang, C., Effects of working parameters on electrospinning, in *One-Dimensional Nanostructures*. Springer. p. 15-28, 2013.
- [42] De Vrieze, S., Van Camp, T., Nelvig, A., Hagstrom, B., Westbroek, P., De Clerck, K., The effect of temperature and humidity on electrospinning. *Journal of Materials Science*, 44(5), 1357-1362, 2009.
- [43] Qu, H., Wei, S., Guo, Z., Coaxial electrospun nanostructures and their applications. *Journal of Materials Chemistry A*, 1(38), 11513-11528, 2013.
- [44] Yarin, A. L., Coaxial electrospinning and emulsion electrospinning of core-shell fibers. *Polymers for Advanced Technologies*, 22(3), 310-317, 2011.
- [45] Lyons, J., Li, C., Ko, F., Melt-electrospinning part I: processing parameters and geometric properties. *Polymer*, 45(22), 7597-7603, 2004.
- [46] Dalton, P. D., Grafahrend, D., Klinkhammer, K., Klee, D., Moller, M., Electrospinning of polymer melts: Phenomenological observations. *Polymer*, 48(23), 6823-6833, 2007.
- [47] Reneker, D., Yarin, A., Zussman, E., Xu, H., Electrospinning of nanofibers from polymer solutions and melts. *Advances in applied mechanics*, 41, 43-346, 2007.
- [48] Sun, Z., Zussman, E., Yarin, A. L., Wendorff, J. H., Greiner, A., Compound core-shell polymer nanofibers by co-electrospinning. *Advanced materials*, 15(22), 1929-1932, 2003.
- [49] Zhang, Y. Z., Wang, X., Feng, Y., Li, J., Lim, C. T., Ramakrishna, S., Coaxial electrospinning of (fluorescein isothiocyanate-conjugated bovine serum albumin)-encapsulated poly(epsilon-caprolactone) nanofibers for sustained release. *Biomacromolecules*, 7(4), 1049-1057, 2006.

- [50] Yu, J. H., Fridrikh, S. V., Rutledge, G. C., Production of submicrometer diameter fibers by two-fluid electrospinning. *Advanced Materials*, 16(17), 1562-+, 2004.
- [51] Diaz, J. E., Barrero, A., Marquez, M., Loscertales, I. G., Controlled encapsulation of hydrophobic liquids in hydrophilic polymer nanofibers by co-electrospinning. *Advanced Functional Materials*, 16(16), 2110-2116, 2006.
- [52] Elahi, M. F., Lu, W., Guoping, G., Khan, F., Core-shell Fibers for Biomedical Applications-A Review. *J Bioengineer & Biomedical Sci* 3: 121. doi, 2013.
- [53] Loscertales, I. G., Barrero, A., Guerrero, I., Cortijo, R., Marquez, M., Ganan-Calvo, A. M., Micro/nano encapsulation via electrified coaxial liquid jets. *Science*, 295(5560), 1695-1698, 2002.
- [54] Zhang, Y. Z., Huang, Z. M., Xu, X. J., Lim, C. T., Ramakrishna, S., Preparation of core-shell structured PCL-r-gelatin Bi-component nanofibers by coaxial electrospinning. *Chemistry of Materials*, 16(18), 3406-3409, 2004.
- [55] Zhang, Y. Z., Venugopal, J., Huang, Z. M., Lim, C. T., Ramakrishna, S., Characterization of the surface biocompatibility of the electrospun PCL-collagen nanofibers using fibroblasts. *Biomacromolecules*, 6(5), 2583-2589, 2005.
- [56] Huang, Z. M., He, C. L., Yang, A. Z., Zhang, Y. Z., Hang, X. J., Yin, J. L., Wu, Q. S., Encapsulating drugs in biodegradable ultrafine fibers through co-axial electrospinning. *Journal of Biomedical Materials Research Part A*, 77a(1), 169-179, 2006.
- [57] Jiang, H. L., Hu, Y. Q., Li, Y., Zhao, P. C., Zhu, K. J., Chen, W. L., A facile technique to prepare biodegradable coaxial electrospun nanofibers for controlled release of bioactive agents. *Journal of Controlled Release*, 108(2-3), 237-243, 2005.
- [58] Jiang, H. L., Hu, Y. Q., Zhao, P. C., Li, Y., Zhu, K. J., Modulation of protein release from biodegradable core-shell structured fibers prepared by coaxial electrospinning. *Journal of Biomedical Materials Research Part B-Applied Biomaterials*, 79b(1), 50-57, 2006.
- [59] Saraf, A., Baggett, L. S., Raphael, R. M., Kasper, F. K., Mikos, A. G., Regulated non-viral gene delivery from coaxial electrospun fiber mesh scaffolds. *Journal of Controlled Release*, 143(1), 95-103, 2010.
- [60] Liao, I. C., Chen, S. L., Liu, J. B., Leong, K. W., Sustained viral gene delivery through core-shell fibers. *Journal of Controlled Release*, 139(1), 48-55, 2009.
- [61] Khalf, A., Singarapu, K., Madihally, S. V., Cellulose acetate core-shell structured electrospun fiber: fabrication and characterization. *Cellulose*, 22(2), 1389-1400, 2015.

- [62] Yu, D. G., Branford-White, C., Bligh, S. W. A., White, K., Chatterton, N. P., Zhu, L. M., Improving Polymer Nanofiber Quality Using a Modified Co-axial Electrospinning Process. *Macromolecular Rapid Communications*, 32(9-10), 744-750, 2011.
- [63] Yu, D. G., Chatterton, N. P., Yang, J. H., Wang, X., Liao, Y. Z., Coaxial Electrospinning with Triton X-100 Solutions as Sheath Fluids for Preparing PAN Nanofibers. *Macromolecular Materials and Engineering*, 297(5), 395-401, 2012.
- [64] Yu, D. G., Lu, P., Branford-White, C., Yang, J. H., Wang, X., Polyacrylonitrile nanofibers prepared using coaxial electrospinning with LiCl solution as sheath fluid. *Nanotechnology*, 22(43), 2011.
- [65] Yu, D. G., Williams, G. R., Gao, L. D., Bligh, S. W. A., Yang, J. H., Wang, X., Coaxial electrospinning with sodium dodecylbenzene sulfonate solution for high quality polyacrylonitrile nanofibers. *Colloids and Surfaces a-Physicochemical and Engineering Aspects*, 396, 161-168, 2012.
- [66] Tiwari, S. K., Tzezana, R., Zussman, E., Venkatraman, S. S., Optimizing partition-controlled drug release from electrospun core-shell fibers. *International journal of pharmaceutics*, 392(1), 209-217, 2010.
- [67] Abrigo, M., McArthur, S. L., Kingshott, P., Electrospun nanofibers as dressings for chronic wound care: advances, challenges, and future prospects. *Macromolecular bioscience*, 14(6), 772-792, 2014.
- [68] Shin, Y., Hohman, M., Brenner, M., Rutledge, G., Experimental characterization of electrospinning: the electrically forced jet and instabilities. *Polymer*, 42(25), 09955-09967, 2001.
- [69] Fong, H., Chun, I., Reneker, D. H., Beaded nanofibers formed during electrospinning. *Polymer*, 40(16), 4585-4592, 1999.
- [70] Jarusuwannapoom, T., Hongrojjanawiwat, W., Jitjaicham, S., Wannatong, L., Nithitanakul, M., Pattamaprom, C., Koombhongse, P., Rangkupan, R., Supaphol, P., Effect of solvents on electro-spinnability of polystyrene solutions and morphological appearance of resulting electrospun polystyrene fibers. *European Polymer Journal*, 41(3), 409-421, 2005.
- [71] Jeffrey, G. A., Jeffrey, G. A., An introduction to hydrogen bonding. Vol. 12. 1997: Oxford university press New York.
- [72] Lam, C. X. F., Savalani, M. M., Teoh, S. H., Hutmacher, D. W., Dynamics of in vitro polymer degradation of polycaprolactone-based scaffolds: accelerated versus simulated physiological conditions. *Biomedical Materials*, 3(3), 2008.

[73] Song, S. S., Kim, H. H., Yil, W. Y., Reaction of ethylene oxide polymers with lactides, glycolide and caprolactone. 1996, Google Patents.

[74] Ramteke, K., Mathematical Models of Drug Dissolution: A Review.

[75] Zamani, M., Morshed, M., Varshosaz, J., Jannesari, M., Controlled release of metronidazole benzoate from poly ϵ -caprolactone electrospun nanofibers for periodontal diseases. *European Journal of Pharmaceutics and Biopharmaceutics*, 75(2), 179-185, 2010.

[76] Repanas, A., Glasmacher, B., Dipyrindamole embedded in Polycaprolactone fibers prepared by coaxial electrospinning as a novel drug delivery system. *Journal of Drug Delivery Science and Technology*, 29, 132-142, 2015.

[77] Kataria, K., Gupta, A., Rath, G., Mathur, R., Dhakate, S., In vivo wound healing performance of drug loaded electrospun composite nanofibers transdermal patch. *International journal of pharmaceutics*, 469(1), 102-110, 2014.

[78] Berg, H. C., *Random walks in biology*. 1993: Princeton University Press.

[79] Siepmann, J., Peppas, N. A., Higuchi equation: derivation, applications, use and misuse. *International journal of pharmaceutics*, 418(1), 6-12, 2011.

APPENDIX

A. Derivation of Fick's First and Second Laws of Diffusion

Firstly, a collection of particles performing a random walk is considered. The length scale of the one dimensional walk is Δx and the time scale is Δt . Finally, $N(x,t)$ is the number of particles which is present at position x at time t . At point x , half of the particles would move to the right and at point $x + \Delta x$, half of the particles would move to the left [78]. The net movement to the right can be shown as:

$$-\frac{1}{2} \times (N(x + \Delta x, t) - N(x - t)) \quad (\text{A.1})$$

J (flux) means the net movement of particles through a surface area of A within the time interval Δt . It can be written as:

$$J = -\frac{1}{2} \times (N(x + \Delta x, t) \div A\Delta t - N(x - t) \div A\Delta t) \quad (\text{A.2})$$

If up and down sides of the equation is multiplied by $(\Delta x)^2$:

$$J = -\frac{\Delta x^2}{2\Delta t} (N(x + \Delta x, t) \div A\Delta x^2 - N(x - t) \div A\Delta x^2) \quad (\text{A.3})$$

Concentration (C) is equal to number of particles per unit volume which is $N/(A\Delta x)$ and diffusion constant is expressed as $(\Delta x)^2/(2\Delta t)$. By using those definitions, the equation can be simplified into:

$$J = -D (C(x + \Delta x, t) \div \Delta x - C(x - t) \div \Delta x) \quad (\text{A.4})$$

By taking the limit of the right side:

$$J = -D \frac{dC}{dx} \quad (\text{A.5})$$

Where, D is the diffusion constant, C refers to the concentration and x is the position. This equation gives Fick's first law of diffusion from which Fick's second law can be derived. By considering mass conservation:

$$\frac{\partial C}{\partial t} + \frac{\partial}{\partial x} J = 0 \quad (\text{A.6})$$

By using Fick's first law:

$$\frac{\partial C}{\partial t} - \frac{\partial}{\partial x} \left(D \frac{dC}{dx} \right) = 0 \quad (\text{A.7})$$

And finally Fick's second law of diffusion is described as:

$$\frac{\partial C}{\partial t} = D \frac{\partial^2 C}{\partial x^2} \quad (\text{A.8})$$

Where, D refers to the diffusion constant, t is the time, C is the concentration and x is the position.

B. Derivation of Zero and First Order Release Equations

The differential equation used for describing zero-order drug release kinetics is:

$$\frac{dC}{dt} = k \quad (\text{B.1})$$

Where, t is time, C is the drug concentration and k is the zero order kinetics constant.

After rearrangement:

$$dC = k dt \quad (\text{B.2})$$

After integration:

$$C_t - C_0 = kt \quad (\text{B.3})$$

$$C_t = C_0 + kt \quad (\text{B.4})$$

Where, C_0 is the initial drug concentration, C_t is the drug concentration at a certain time (t) and k is the zero order kinetics constant.

The differential equation used for describing first-order drug release kinetics is:

$$\frac{dC}{dt} = kC \quad (\text{B.5})$$

Where, t is time, C is the drug concentration in release medium and k is the first order kinetics constant. After rearrangement:

$$\frac{dC}{C} = kdt \quad (\text{B.6})$$

After integration:

$$\ln \frac{C_t}{C_0} = kt \quad (\text{B.7})$$

$$\frac{C_t}{C_0} = e^{kt} \quad (\text{B.8})$$

In decimal logarithms:

$$\log C_t = \log C_0 + \frac{kt}{2.303} \quad (\text{B.9})$$

Where, C_0 is the initial drug concentration, C_t is the drug concentration at a certain time (t) and k is the first order kinetics constant.

C. Derivation of Higuchi equation and Peppas equation

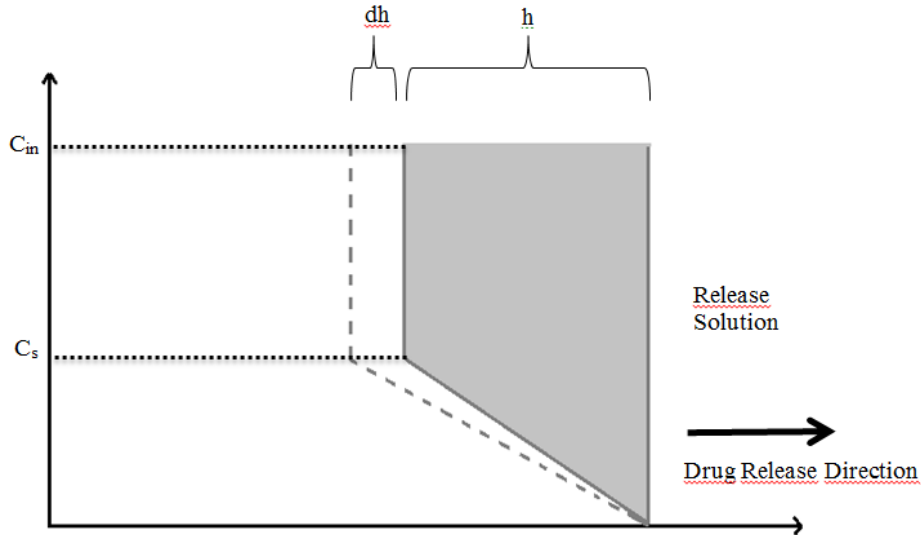


Figure A.1. Schematic illustration of the drug concentration - distance profile of the matrix exposed at time t and $t + dt$.

In Figure A.1, the grey area represents the amount of drug released from the matrix per area. It can be illustrated by the equation [79]:

$$\frac{M_t}{A} = \left(C_{in} - \frac{C_s}{2} \right) \times h \quad (C.1)$$

Where, M_t is the drug released from the matrix at time t , C_{in} refers to the initial drug concentration, C_s represents the drug solubility, and h is the distance of the front. The cumulative amount of drug released per unit surface area dM/A in the time interval dt can be shown as:

$$\frac{dM}{A} = C_{in} \times dh - \frac{C_s}{2} \times dh \quad (C.2)$$

If Fick's 1st law of diffusion is used and a saturated drug solution is considered:

$$\frac{dM}{dt} = A \times D \frac{C_s}{h} \quad (C.3)$$

Where, D is the diffusion coefficient and h is the distance from the surface (at perfect sink conditions). By combining equation (C.2) and (C.3):

$$h = 2 \sqrt{\frac{DtC_s}{2C_{in}-C_s}} \quad (C.4)$$

By substituting equation (C.4) into equation (C.1):

$$\frac{M_t}{A} = \sqrt{(2C_{in} - C_s)DtC_s} \quad (C.5)$$

If C_{in} is much greater than C_s the equation can be simplified to:

$$\frac{M_t}{A} = \sqrt{(2C_{in}DtC_s)} \quad (C.6)$$

If A, C_{in} , D and C_s are taken as constant, the final equation found is:

$$M_t = k_H \sqrt{t} = k_H t^{1/2} \quad (C.7)$$

However, Higuchi equation is used to describe the release from a carrier matrix with thin planar geometry and it was suitable for Fickian diffusion mechanism [79]. It was not applicable for cylinders and spheres. Another equation was proposed by Peppas for modelling the drug release from different carrier matrixes and which is also acceptable for non-Fickian diffusion. The more generic equation proposed by Peppas is:

$$\frac{M_t}{M_\infty} = kt^n \quad (C.8)$$

The n value in this equation was used for characterizing different release mechanisms. For cylindrical shaped matrix, $n=0.45$ means Fickian diffusion and n values between 0.45 and 0.89 refers to non-Fickian diffusion mechanism. The k value is the rate constant which depends on the geometrical shape of the matrix [29].

CURRICULUM VITAE

Personal Information

Surname, Name : SULTANOVA, Zahida
Nationality : Azerbaijani
Date and Place of Birth : 02.12.1990, Azerbaijan
Marital Status : Single
Telephone : 00905544194847
Email : zahidasultanova@gmail.com

Education

Level	Training Unit	Graduation Date
Master Degree	TOBB University of Economics and Technology	2015
Bachelor Degree	Middle East Technical University	2013

Job Experience

Year	Place	Duty
2012	Ankara University	Internship
2014-2015	TOBB University of Economics and Technology	Scholarship Student

Foreign Language

English (Advanced)
Turkish (Advanced)
German (Intermediate)

Publications

- Sultanova, Z., Kabay, G., Kaleli, G., & Mutlu, M., Coaxial electrospun PCL/PVA-chitosan nanofibers: A novel non-viral gene delivery scaffold. In Plasma Sciences (ICOPS), 2015, IEEE International Conference on (pp. 1-1). IEEE.
- Preparation of Enzyme- carrying Living Membranes Produced by Electrospinning for Biosensor Applications, Kabay G., Kaleli G., Sultanova Z., Seker U.O. S., Mutlu M., 2nd International Congress on Biosensors, Gediz University (2015).

- Performance of Enzyme Immobilisation Methods on Bio-inspired Albumin Scaffolds, Kabay G., Kaleli G., Sultanova Z., Seker U.O. S., Mutlu M., NART, (2015).